Critical and off-critical conformal analysis of the Ising quantum chain in an imaginary field

1991 J. Phys. A: Math. Gen. 24 5371

(http://iopscience.iop.org/0305-4470/24/22/021)

J Phys A Math Gen 24 (1991) 5371-5399 Printed in the UK

Critical and off-critical conformal analysis of the Ising quantum chain in an imaginary field

G von Gehlen†

Laboratoire de Physique Théorique et Hautes Energies, Université Paris VI, Paris, France

Received 20 March 1991

Abstract The critical curve with central charge $c = -\frac{22}{5}$ of the Ising quantum chain in an imaginary longitudinal field is calculated by finite-size extrapolation of the Yang–Lee square root branch point position Various power laws are found The field dependence of the off-criticality mass scale and the four lowest off-criticality scaling functions are calculated The latter turn out to be universal along the critical line and agree very well with the results of the truncated Hilbert space method for the $c = -\frac{22}{5}$ continuum theory We obtain the universal bulk scaling coefficient in qualitative agreement with the thermodynamic Bethe ansatz result The scattering phaseshift calculated by Luscher's method reproduces the Cardy–Mussardo minimal solution for the S-matrix If a boundary defect is introduced, the only non-trivial primary field decouples, so that the spectrum consists only of the tower of the unit operator In the antiferromagnetic regime with a non-staggered imaginary field we find boundary-dependent lines where the gap vanishes

1. Introduction

In 1952, Yang and Lee [1], in an attempt to get new insight into the mechanism producing the phase transition in the Ising model, studied the distribution of the zeros of the partition function in the complex plane of an applied magnetic field variable $\mathscr{H}$. They found that these zeros are restricted to a part of the imaginary $\mathscr{H}$-axis In the thermodynamic limit the zeros become dense for $|\mathrm{Im}\ \mathscr{H}| > h_c(T)$, producing 'edge singularities' at positions $\mathscr{H} = \pm i h_c(T)$ which depend on the temperature T. For T above the critical temperature T_c of the system without field $\mathscr{H}$, on the imaginary $\mathscr{H}$ axis there is a gap $|\mathrm{Im}\ \mathscr{H}| \leqslant h_c(T)$ which is free of zeros This gap shrinks to zero when $T \to T_c$.

Subsequently, starting in 1967, several authors [2–11] showed that the situation is analogous for a large class of models. However, while for spherical models the nature of the singularity at $h_c(T)$ is of the square root type for any dimensionality d, for Ising-type models it is strongly d dependent [9]

In 1978, Fisher [12] pointed out that this Yang–Lee singularity can be considered as an ordinary second-order phase transition in an imaginary field $\mathscr{H} = ih$, and that around $d = 6$ [13, 14] its universality class may be described by a Landau–Ginzburg action involving a single scalar field ϕ and an imaginary ϕ^3 coupling:

$$\mathscr{A} = \int [\tfrac{1}{2}(\partial\phi)^2 - i(h - h_c)\phi - ig\phi^3]\, d^d x \tag{1.1}$$

† Permanent address Physikalisches Institut der Universitat, Nussallee 12, D-5300 Bonn 1, Federal Republic of Germany (E-mail Bitnet UNP02F@DBNRHRZ1)

0305-4470/91/225371+29$03 50

The description of this universality class in terms of the powerful tool of conformal field theory (CFT) [15, 16] was established by Cardy [17] in 1985. He showed that in $d=2$ it corresponds to the non-unitary CFT with central charge $c=-\frac{22}{5}$. This CFT is the $p=5$, $q=2$ member of the minimal $M_{p/q}$-series [15], for which the central charge is $c=1-6(p-q)^2/pq$. For $p-q>1$ these theories are non-unitary [15, 18–20] and contain primary fields with negative anomalous dimensions. The $M_{5/2}$ theory has just one non-trivial primary field $\phi_{h,\bar{h}}$ (which is the ϕ of (1 1)) with anomalous dimensions $(h, \bar{h})=(-\frac{1}{5}, -\frac{1}{5})$ The spectra and the modular-invariant partition functions for the $c=-\frac{22}{5}$ theory were calculated in 1986 by Itzykson *et al* [21]

Recently, the principle of conformal invariance has also become an efficient tool for investigating the properties of two-dimensional systems away from criticality [22, 23] One considers the perturbation of the action of conformal theory $\mathscr{A}_{\mathrm{CFT}}$ by an integral over a relevant primary field $\phi_{h,\bar{h}}$

$$\mathscr{A}=\mathscr{A}_{\mathrm{CFT}}+\tau_\phi \int \phi_{h,\bar{h}}(z,\bar{z})\,\mathrm{d}^2 z \tag{1 2}$$

The coupling constant τ_ϕ has dimension $y=2-x$ where $x=h+\bar{h}$

Cardy and Mussardo [24] have applied (1.2) to study the massive theory which arises from the perturbation of the $c=-\frac{22}{5}$ theory by the field $\phi_{(-1/5,-1/5)}$. In this case τ_ϕ has dimension $y=\frac{12}{5}$ and, therefore, going off-criticality, the theory should acquire a mass scale (inverse correlation length) $m\sim\tau_\phi^{5/12}$. Using the Zamolodchikov 'counting argument' [22], in [24] it was shown that the strongly relevant perturbation by $\phi_{(-1/5,-1/5)}$ preserves the integrability, and the S-matrix of the corresponding massive field theory factorizes into elastic two-particle S-matrices The minimal solution for this S-matrix contains only a single type of neutral particles and is explicitly given by [24, 30]

$$S(\theta)=\tanh\left(\frac{\theta}{2}+\frac{1\pi}{6}\right)\coth\left(\frac{\theta}{2}-\frac{1\pi}{6}\right). \tag{1.3}$$

Here $\theta=\theta_1-\theta_2$ is the rapidity difference of the two scattering particles, and the rapidity θ_i $(i=1, 2)$ of each particle is defined in terms of its momentum P_i by $\theta_i=\sinh^{-1}(P_i/m)$

Instead of considering this theory in the two-dimensional plane, using the logarithmic mapping $w=u+\mathrm{i}v=(R/2\pi)\ln z$ it can be studied on a strip of width R in the v-direction [25, 29]. Then it is described by the Hamiltonian (or logarithm of the transfer matrix) H_ϕ:

$$H_\phi=\frac{2\pi}{R}\left(L_0+\bar{L}_0-\frac{c}{12}\right)+\tau_\phi\int_0^R \mathrm{d}v\,\phi_{(-1/5,-1/5)}(w,\bar{w}) \tag{1 4}$$

where L_0 and $\bar{L}_0$ are Virasoro generators of the conformal theory. The eigenvalues E_i of H_ϕ can be written in the scaling form

$$E_i=\frac{2\pi}{R}\mathscr{F}_i(\mu_\phi) \tag{1.5}$$

with the dimensionless scaling variable

$$\mu_\phi\equiv mR\sim R\tau_\phi^{5/12}. \tag{1.6}$$

Yurov and Zamolodchikov [25, 26] have recently computed the scaling functions f_i for the lowest levels of H_ϕ non-perturbatively by truncating the conformal Hilbert

space (see also [29]). The ground state has been calculated using the thermodynamic Bethe ansatz [26–28]. A detailed analysis of the two-point function is given in [31].

While in [17, 24–26, 31] the Lee–Yang edge singularity was studied in the continuum field theory, in the present paper we shall investigate this singularity as it is realized by the Ising quantum chain in the presence of a purely imaginary longitudinal field h, i e. we are going to study the Hamiltonian

$$H = -\tfrac{1}{2}\sum_{i=1}^{N} (\sigma_i^z + \lambda\sigma_i^x\sigma_{i+1}^x + \mathrm{i}h\sigma_i^y) \tag{1.7}$$

where σ_i^x and σ_i^z are Pauli matrices acting at site i, N is the number of sites and λ is the inverse temperature. The phase diagram of (1.7) has a whole phase transition line with $c = -\frac{22}{5}$ (see figure 1). For $h = 0$ H commutes with the Z_2 charge operator so that the spectrum separates into two charge sectors $Q = 0, 1$. For $h \neq 0$ this symmetry is broken. Earlier numerical work on the Hamiltonian (1.7) has been performed in 1979–1981 by Uzelac *et al* [32–35] using the renormalization group blocking method.

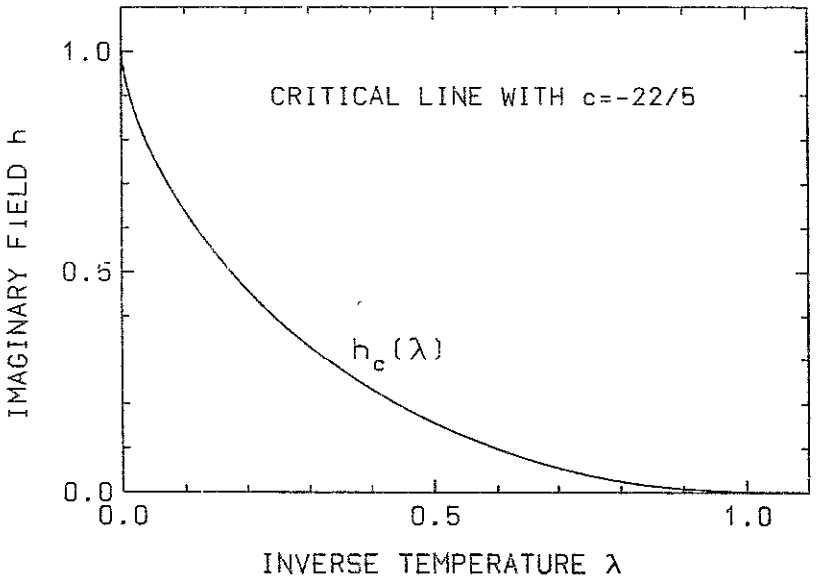

Figure 1. The $c = -\frac{22}{5}$ phase transition curve $h_c(\lambda)$ calculated from finite-size scaling of the square root branch point positions.

A particularly interesting aspect of the Hamiltonian (1.7) is the presence of *two* dimensionful parameters, λ and h, whereas there is only one relevant primary perturbing field. This will allow us to make several non-trivial crosschecks of the results obtained, since many ways of going off-critical should be equivalent. Furthermore, the off-criticality region of the $c = -\frac{22}{5}$ line has to join to the thermally perturbed standard Ising model at $h = 0$ where the spectrum and the S-matrix are explicitly known (there $S(\theta) = -1$, independent of θ [36]).

Apart from its critical and off-criticality properties we shall also consider the dependence of the critical spectrum on smooth changes of the boundary condition

(BC), which we assume to be of the form

$$\sigma_{N+1}^{x} = a\sigma_1^x \tag{1.8}$$

with a real parameter a. This includes the periodic, free and antiperiodic BC cases for $a = 1, 0, -1$, respectively. We shall see that only for $a \leq 1$ the Yang–Lee singularity converges for $N \to \infty$ to the critical line. For $a > 1$ it moves to the massive region.

This paper is organized as follows. In section 2 we present the calculation of the critical curve from finite-size scaling of the square-root branch point position. Then in section 3 we study the off-criticality scaling behaviour and calculate the elastic scattering phaseshift of the massive theory. Section 4 deals with the boundary condition dependence of the spectrum and section 5 gives results about the presence of a Yang–Lee-type singularity in the antiferromagnetic region. Section 6 summarizes our conclusions.

2. The Yang–Lee singularity for periodic boundary condition

2.1. Determination of the $c = -\frac{22}{5}$ critical curve from the lowest-level crossings

In this section we present our numerical results on the critical behaviour of the Hamiltonian (1.7) with periodic boundary condition, i.e. $a = 1$ in (1.8).

H of (1.7) has the special property that, although it is non-Hermitian, its eigenvalues are not complex everywhere but in a restricted region of the (λ, h)-plane, they remain real. In order to see the origin of this property consider $H' = AHA^{-1}$ with $A = \exp(i\pi\sigma_z/4)$, which replaces $\sigma_i^x \to -\sigma_i^y$ and $\sigma_i^z \to \sigma_i^z$. Then H' is a real but non-symmetric matrix. Its characteristic polynomial (and also that of H) has real coefficients and so the eigenvalues are either real or come in complex conjugate pairs. H is symmetric but non-Hermitian, and the spectrum does not change if we replace $h \to -h$.

For $h = 0$ the eigenvalues are real, and if they are non-degenerate, in going to $h \neq 0$ they cannot form complex conjugate pairs before they cross another level. Since in the high-temperature region ($\lambda < 1$) the lowest eigenvalues stay non-degenerate in the thermodynamic limit, there we have a finite range of $|h|$ where the lowest eigenvalues are real.

We determine position of the Yang–Lee–Fisher phase transition from the first crossing $h_c(\lambda, N)$ of the two lowest levels for $N = 2, \ldots, 19$ sites and estimate the limit $N \to \infty$ using both a Van-den-Broeck–Schwartz algorithm [37] and the extrapolation by rational approximants [38, 39]. In the second column of table 1 we give the limiting values

$$h_c(\lambda) = \lim_{N\to\infty} h_c(\lambda, N) \tag{2.1}$$

for several values of the inverse temperature λ. The use of the Lanczos diagonalization method made it possible to go up to $N = 19$ sites. For this we adapted the Lanczos algorithm to the case of a non-Hermitian but symmetric matrix by redefining the scalar product to be $\langle u, v\rangle = \Sigma_i u_i v_i$ instead of the usual $\Sigma_i u_i^* v_i$. Sometimes problems of stability arise in this generalized Lanczos procedure; however, in practice often these can be overcome comparing the convergence for different starting vectors. For small values of λ, i.e. $\lambda \leq 0.02$, these instabilities make Lanczos calculations for $N \geq 14$ unreliable.

Table 1. Critical imaginary fields h_c, conformal normalization ξ and coefficient B of the approach of $h_c(\lambda, N)$ to $h_c(\lambda)$ as defined in (2.6), for various values of the inverse temperature λ. a_0 is the leading bulk coefficient, $a_0(\lambda, \tau=0)$, defined in (2.3). The figures in parentheses give our estimate of the uncertainty in the last given digit.

λ	$h_c(\lambda)$	$\xi(\lambda)$	$\xi(\lambda)/\lambda^{5/12}$	$B(\lambda)$	$a_0(\lambda)$
0.002	0.970 715 (1)	0.097	1.29	0.029 75 (2)	0.092 21 (3)
0.005	0.946 362 (1)	0.1315	1.196	0.055 1 (1)	0.124 52 (2)
0.01	0.915 479 (1)	0.166	1.13	0.088 6 (1)	0.156 01 (1)
0.02	0.867 409 (4)	0.21	1.07	0.143 7 (2)	0.194 92 (3)
0.05	0.762 430 (2)	0.292	1.017	0.278 6 (1)	0.259 377 (2)
0.10	0.636 640 (3)	0.376	0.981	0.474 1 (2)	0.319 12 (2)
0.15	0.539 1777 (3)	0.4390	0.9677	0.601 3 (1)	0.358 642 (5)
0.20	0.458 498 (1)	0.49	0.96	0.850 0 (3)	0.388 698 (5)
0.30	0.330 031 (2)	0.582	0.961	1.252 (3)	0.434 295 (3)
0.40	0.232 02 (1)	0.657	0.962	1.714 (6)	0.469 64 (3)
0.50	0.156 20 (2)	0.721	0.962	2.265 (5)	0.499 782 (4)
0.60	0.098 07 (2)	0.773	0.956	2.97 (1)	0.527 21 (3)
0.70	0.054 83 (3)	0.842	0.977	3.93 (4)	0.553 49 (2)
0.80	0.024 68 (2)	0.890	0.977	5.50 (6)	0.579 75 (3)
0.85	0.014 13 (5)			6.78 (8)	
0.90	0.006 5 (2)				

With increasing N the $h_c(\lambda, N)$ converge from above (for the positive h_c) to their limiting values†: so the finite-size spectra $\mathscr{E}_i$ at $h_c(\lambda)$

$$\mathscr{E}_i(\lambda, h_c) = \lim_{N\to\infty} \frac{N}{2\pi\xi(\lambda)} (E_i(\lambda, h_c, N) - E_{\text{vac}}(\lambda, h_c, N)) = x_i \tag{2.2}$$

(where E_{vac} is the vacuum energy) are real and can be used to calculate the corresponding anomalous dimensions x_i. In (2.2) $E_0, E_1, E_2, \ldots$ are the lowest eigenvalues of H. $\xi(\lambda)$ is the conformal normalization factor, to be determined from the spacing of the lowest momentum gap, see [41]. Recall that for $h = h_c(\lambda)$ in general $H/\xi(\lambda)$, not H itself, converges to H_ϕ of (1.3) in the continuum limit.

The central charge c is obtained from the N dependence of the vacuum energy E_{vac} [40]:

$$E_{\text{vac}}(\lambda, h_c, N) = -Na_0 + a_1 - \frac{\tilde{c}\pi}{6N} + \ldots \tag{2.3}$$

where $\tilde{c} = c\xi$ for the periodic BC and $\tilde{c} = c\xi/4$ for the free BC [40]. For the periodic BC, in addition, we have $a_1 = 0$.

We have calculated the 15 lowest levels of the spectrum for various values of λ. As expected [21], for $\lambda < 1$ the *second* level E_1 corresponds to the vacuum and gives $c = -\frac{22}{5}$. From the lowest gap $E_0 - E_1$ we get $\mathscr{E}_0 = -\frac{2}{5}$, which is the dimension of the primary field $\phi_{(-1/5,-1/5)}$. The higher levels order into the towers of the unit operator and of $\phi_{(-1/5,-1/5)}$, in agreement with the transfer matrix results of [21], so that we

† We have checked that this is the case for $\lambda \leqslant 0.3$ for the 10 lowest zero-momentum levels. For $\lambda \geqslant 0.5$ the fourth and fifth levels cross below h_c and the convergence of the crossing points to h_c is from below. The lower-level crossings near h_c occur between the pair of levels belonging to $x = -\frac{2}{5} + n$ and $x = 0 + n$, $n = 0, 2, 4$. Since there is no level $x = 0 + 2$, the level $x = -\frac{2}{5} + 2$ has no partner and stays real around h_c.

shall not reproduce the numbers here. However, for the quantum chain one needs also the conformal normalization factor $\xi(\lambda)$ on the $c=-\frac{22}{5}$ curve. We list our results for $\xi(\lambda)$ in the third column of table 1. The fourth column of the same table shows that, except for the region of λ below 0.1, we have $\xi \approx \lambda^{5/12}$ with corrections of only a few per cent This qualitative property will be useful later in section 4. For very small λ the data suggest $\xi \approx (0.77 \pm 0.01)\lambda^{1/3}$. For the Ising case $h=0$, $\lambda=1$ it is known that $\xi=1$ [41].

For $\lambda \geqslant 1$ we obtain $h_c(\lambda)=0$ because in the low-temperature phase the ground state of the field-free Ising model becomes degenerate in the limit $N \to \infty$.

2.2 *Power laws and scaling at the Yang–Lee singularity*

We now study more in detail how in (2.1) and (2.2) the limit $N \to \infty$ is approached from finite N. We shall concentrate on the lowest gap.

Since for finite N in the range $0<\lambda<\infty$ we find no triple crossing of the lowest levels, the resulting branch points are of the square root type So we write for ΔE, the gap between the two lowest eigenvalues:

$$\Delta E(\lambda, h, N) = E_0 - E_1 = A(\lambda, h, N)\sqrt{h_c(\lambda, N) - h}. \tag{2.4}$$

For $h \to h_c(\lambda, N)$ our data for $A(\lambda, h, N)$ at fixed λ show a clear leading power behaviour for the N dependence. Including also a non-leading dependence on $\Delta h_{\lambda,N} = h_c(\lambda, N) - h$, we write

$$A(\lambda, h, N) = (A(\lambda) + A_1(\lambda, N)\Delta h_{\lambda,N})N^{-\alpha} + \ldots \tag{2.5}$$

Similarly, the leading N dependence of the approach of $h_c(\lambda, N)$ to its limiting value $h_c(\lambda)$ fits to the form

$$h_c(\lambda, N) - h_c(\lambda) = B(\lambda)N^{-\beta} + \ldots \tag{2.6}$$

Inserting (2.5) and (2.6) into (2.4) and neglecting $A_1(\lambda, N)$. we get the leading behaviour of the gap near the critical curve:

$$\Delta E(\lambda, h, N) = A(\lambda)N^{-\alpha-\beta/2}\sqrt{(h_c(\lambda) - h)N^{\beta} + B(\lambda) + \ldots} + \ldots \tag{2.7}$$

For $h = h_c(\lambda)$ we can use the result (2.2) of conformal invariance

$$\lim_{N\to\infty} N\Delta E(\lambda, h_c(\lambda), N) = 2\pi x \xi(\lambda) \tag{2.8}$$

where x is the dimension of the operator giving the transition between the two lowest levels Comparing (2.7) and (2.8) we see that we must have

$$\alpha + \beta/2 = 1 \tag{2.9}$$

and

$$A(\lambda)\sqrt{B(\lambda)} = 2\pi x \xi(\lambda) \tag{2.10}$$

From our numerical data (see table 2) we find that for $0<\lambda<1$ we have $\beta=\frac{12}{5}$ or $2\alpha = -\frac{2}{5}$. For the Ising point $\lambda=1$, $h=0$ we get $\beta=\frac{15}{8}$ or $2\alpha=\frac{1}{8}$. So $2\alpha = x_m$, where x_m is the dimension of the lowest primary field.

In analogy to (1.5) we introduce the scaling variable μ_h,

$$\mu_h = (h_c(\lambda) - h)N^{2-x_m} \tag{2.11}$$

Table 2 Branch point positions $h_c(\lambda, N)$ for periodic chains of finite size N, approximants to the exponents β, (2.6), calculated from N and $N+1$ sites, and slope A of the lowest gap at the branch point, (2.5), for a typical value on the $c=-\frac{22}{5}$ curve and for the Ising case

	$\lambda=0.15$			$\lambda=1.00$	
N	$h_c(N)$	$\beta(N)$	$A(N)$	$h_c(N)$	$\beta(N)$
2	0.644 960 1938	2.201 466	1.371 005	0.225 711 998 47	1.951 0405
3	0.582 504 4281	2.276 255	1.371 083	0.102 327 759 38	1.911 6596
4	0.561 687 0767	2.318 472	1.371 167	0.059 040 932 28	1.896 6913
5	0.552 595 4683	2.343 088	1.370 950	0.038 607 387 62	1.889 3618
6	0.547 930 5931	2.358 351	1.370 678	0.027 399 510 91	1.885 2182
7	0.545 262 7979	2.368 358	1.370 43	0.020 48[illegible]601 12	1.882 6447
8	0.543 612 9883	2.375 232	1.370 23	0.015 935 117 51	1.880 9360
9	0.542 530 6165	2.380 138	1.370 06	0.012 768 522 60	1.879 7432
10	0.541 786 9374	2.383 752	1.369 93	0.010 474 379 82	1.878 8774
11	0.541 256 6483	2.386 487	1.369 82	0.008 757 023 95	1.878 2290
12	0.540 866 8250	2.388 603	1.369 73	0.007 436 712 06	1.877 7308
13	0.540 572 8758	2.390 272	1.369 66	0.006 398 926 00	1.877 3397
14	0.540 346 3886	2.391 619		0.005 567 824 06	1.877 0271
15	0.540 168 6191	2.392 684		0.004 891 518 74	1.876 7732
16	0.540 026 8302	2.393 604		0.004 333 513 61	1.876 5642
17	0.539 912 1348	2.394 369		0.003 867 516 8	1.876 3901
18	0.539 818 168	2.394 769		0.002 474 189 4	1.876 2307
19	0.539 740 4			0.003 139 045	
∞	0.539 177 7 (3)	2.400 4 (5)	1.36 (1)	−0.000 004 (6)	1.875 00 (3)

and see that for fixed λ and small off-criticality (small μ_h) the inverse correlation length $\zeta^{-1}\equiv|\Delta E|$ depends on N and $h-h_c$ only through the factor N^{-1} and μ_h:

$$\Delta E(\lambda, h, N)=\frac{2\pi x\xi(\lambda)}{N}\sqrt{1+\frac{\mu_h}{B(\lambda)}+\ldots}+\ldots \tag{2.12}$$

We list our numerical results for $B(\lambda)$ in the fifth column of table 1. $A(\lambda)$ can then be obtained from (2.10). Observe that for the Ising case $\lambda=1$ approximately we have $A=\sqrt{B}=\sqrt{\pi/4}$. Of course, we find $h_c(\lambda=1)=0$, which is the Yang–Lee mechanism for the Ising phase transition. For $\lambda>1$, i.e. for temperatures below the critical point, $h_c(\lambda)$ is zero, as it should be: there the eigenvalues become complex already for small imaginary fields.

For the particular value $\lambda=0.15$ we have also estimated second-order corrections to (2.4) and (2.6). We find that $A_1(\lambda, N)$, the leading deviation from the simple square root behaviour of ΔE, is approximately $A_1(\lambda, N)=0.04\,N^{2.4}$ for large N, so that

$$A_1(\lambda, N)\Delta h=A_1(\lambda)\mu_h \tag{2.13}$$

with μ_h being the scaling variable of (2.11). The next-order correction to (2.6) for $\lambda=0.15$ turns out to behave like $N^{-4.4}$. For this value of λ an improved form of (2.6) is

$$h_c(\lambda=0.15, N)-0.539\,1777\,(3)=0.6612\,(1)N^{-2.4}-0.572\,(4)N^{-4.4}+\ldots. \tag{2.14}$$

The corrections to (2.6) for the Ising case can be summarized, writing

$$h_c(\lambda=1, N)=\left(\frac{\pi}{4}-0.001\,60\,(1)\right)N^{-1.875}+0.1668\,(2)N^{-3.875}+\ldots \tag{2.15}$$

The slope of the $c=-\frac{22}{5}$ critical curve near $\lambda=1$ is highly consistent with the formula

$$h_c(\lambda)=\tfrac{1}{2}(1-\lambda)^{15/8}+\ldots. \tag{2.16}$$

The exponent in this formula has been determined earlier by Uzelac *et al* to be 1.8 ± 0.1 (see (18) of [32]). Near $\lambda=0$, we find $h_c\approx 1-1\,87\,(4)\lambda^{2/3}$ and $B\approx(1.875\pm0.003)\lambda^{2/3}$. $A(\lambda, N)$ increases only slowly from -1.41 to $-1\,29$ when λ goes from 0 to 0.4. For $\lambda\to 1$ it steeply approaches zero

All the above determinations of the critical curve were done at fixed λ We have also checked that the same exponents are obtained if we look instead for the branch point $\lambda_c(h, N)$ along fixed h. For example, at the fixed value $h=0.539\,18$ we find again $\beta=\frac{15}{8}$ and $\lambda_c(h)=\lim_{N\to\infty}\lambda_c(h, N)=0.149\,999\,(1)$. Defining $B_\lambda(h)$ by

$$\lambda_c(h, N)-\lambda_c(h)=B_\lambda(h)N^{-2\,4}+\ldots \tag{2.17}$$

we get $B_\lambda(h=0.539\,18)=0.375\,83\,(4)$ So, at $\lambda=0.15$, using $B=0\,6613\,(1)$ from table 1, we have $B/B_\lambda=1\,760\,(1)$, which agrees well with the slope of the critical curve at $\lambda=0.15$, which we find to be $\mathrm{d}h/\mathrm{d}\lambda=-1.758$.

3. Off-criticality scaling properties

The off-criticality behaviour of the continuum $c=-\frac{22}{5}$ theory has been studied in [24–26]. However, no detailed information is available which shows how the continuum results compare to the off-criticality properties of a lattice version of this theory. In the following, we give such a comparison for the chain Hamiltonian realization (1.7).

In the (λ, h) plane, the Hamiltonian (1.7) has a whole line which for $N\to\infty$ realizes the $c=-\frac{22}{5}$ theory. This opens the interesting possibility of performing various independent comparisons between the continuum results and the properties of the chain (1.7). Recently, the off-criticality behaviour of several other quantum chains has been investigated (see [42–48]). Two-dimensional lattice models off-criticality have been studied by Monte Carlo simulations [49, 50].

3.1. The mass gap

We start giving the results for the mass scale m of the massive theory, which we define by the lowest gap E_1-E_0:

$$m=E_1-E_0. \tag{3.1}$$

We fix the normalization of m by writing the Hamiltonian in the form (1.7).

Since there is only one relevant perturbation $\phi_{(-1/5,-1/5)}$ to bring us from the critical curve with $c=-\frac{22}{5}$ into the massive high-temperature phase, in all directions down to the left in figure 1 the lowest gap should increase like

$$m\sim\tau^{5/12} \tag{3.2}$$

where τ is the distance from the critical curve in the (λ, h) plane. Since a particular point in the massive region can be reached from different points on the critical curve by choosing different directions, by consistency, the variation of the proportionality constant in (3.2) is determined by the slope of the critical curve. For example, choosing τ first horizontal $(\tau_h=\lambda_c-\lambda)$ and then vertical $(\tau_v=h_c-h)$ in figure 1, we write

$$\begin{aligned} m(\lambda, h)&=a_h(\lambda)(\lambda_c-\lambda)^{5/12}\\ &=a_v(\lambda)(h_c-h)^{5/12} \end{aligned} \tag{3.3}$$

which for small τ gives

$$\frac{a_h(\lambda)}{a_v(\lambda)} = \left(-\frac{dh}{d\lambda}\right)^{5/12} \tag{3.4}$$

and similarly for other directions. Equation (3.4) is excellently confirmed by our numerical data: e.g. for $\lambda = 0.15$ we find $a_v = 1.556\,(1)$ and $a_h = 1.97\,(1)$ which fits well with $dh/d\lambda(\lambda = 0.15) = 1.758$, which we obtain from the slope of the critical curve (compare also the discussion of the ratio B/B_λ after (2.17)). So, in the following we shall consider only the vertical off-criticality direction with constant λ.

In the lattice model (1.7) which we are considering, the power law (3.2) cannot be valid for large values of τ because the phase diagram is symmetric with respect to $h \to -h$, so that we expect the slope $dm/d\tau$ to vanish at $h = 0$. Since from the Ising chain solution we know that the gap is $m = 1 - \lambda$ at $h = 0$, for small h and constant λ we expect $m = 1 - \lambda + d_0 h^2$. Numerically we find $d_0 = 1.1339\,(2)$, $1.4673\,(3)$, $2.468\,(1)$ for $\lambda = 0.15$, 0.20, 0.30, respectively. Plotting our numerical results for $m/(1-\lambda)$ at fixed λ against $1 - h/h_c$ in figure 2, we see that for a broad range of λ the data lie almost on top of each other and approximately form an arc of a circle.

In order to get a more sensitive picture of the behaviour of m at fixed λ for small values of $\tau_v = h_c - h$, in figure 3 we show a logarithmic plot of $a_v(\lambda, \tau_v)$ for various values of λ. This is calculated *not* taking into account the conformal normalization ξ which is strongly λ dependent, but just using the gap as it is normalized in (1.7). For $\tau_v \to 0$ the values of m calculated this way show only a slow variation with respect to λ. We find $a_v(\lambda, \tau_v = 0) = 1.368\,(4)$, $1.487\,(2)$, $1.556\,(1)$, $1\,56\,(1)$ and $1.53\,(2)$ for $\lambda = 0.01$, 0.05, 0.15, 0.30 and 0.50, respectively.

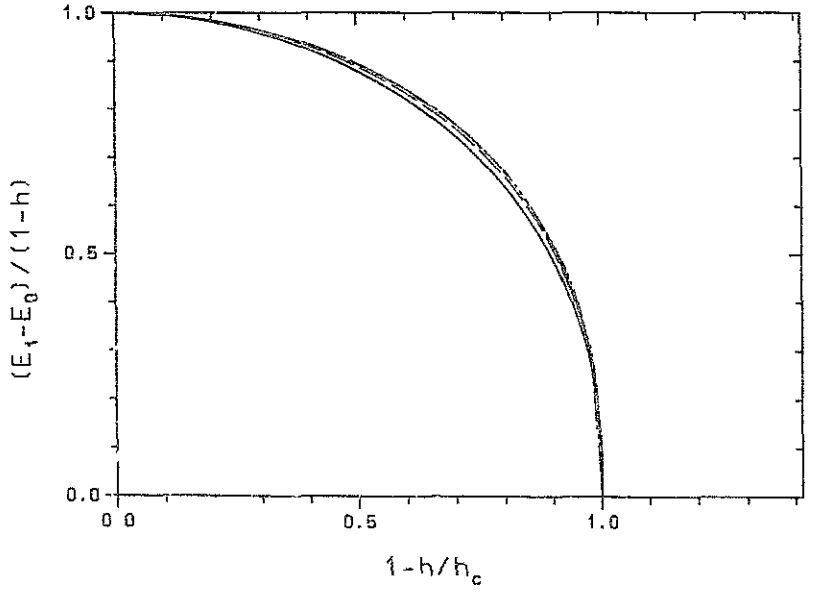

Figure 2. Lowest gap in the off-critical region, normalized to the $h = 0$ Ising gap $1 - \lambda$. Among the various curves for different values of λ, one can distinguish the full line for $\lambda = 0\,01$ and the broken line for $\lambda = 0\,05$. The other curves for $\lambda = 0.15$, $0\,30$ and $0\,50$ fall practically on top of each other on this scale.

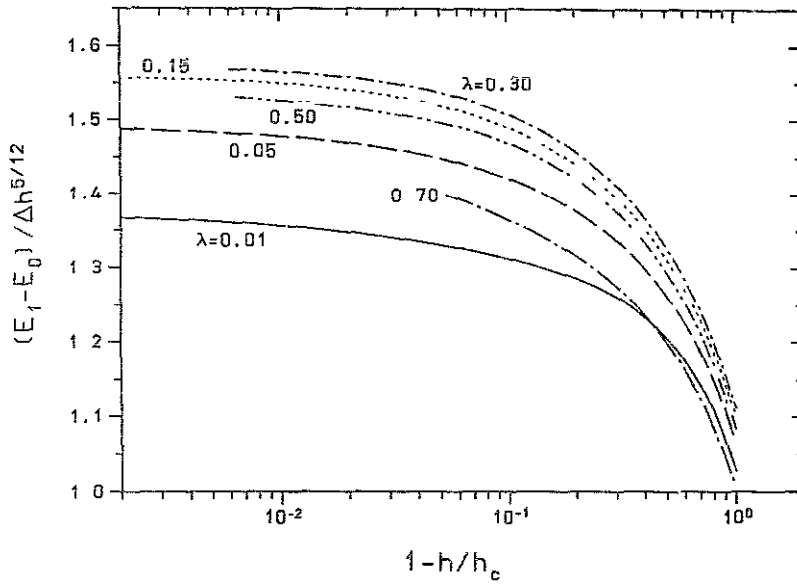

Figure 3. Lowest gap in the off-critical region, normalized by the leading power dependence near h_c, for several fixed values of λ. The right-most point of the curves corresponds to $h=0$, i.e. the Ising value.

If, instead of normalizing m according to (1.7), we use the conformal normalization then, because for $\lambda \geq 0.02$ we have $\xi \approx \lambda^{5/12}$, it is useful to write

$$\frac{m}{\xi} = \tilde{a}_v(\lambda)\left(\frac{\Delta h}{\lambda}\right)^{5/12} \tag{3.5}$$

and we find that $\tilde{a}_v$ too is only weakly λ dependent. In fact, we get $\tilde{a}_v = 1.21\,(1)$, 1.46 (1), 1.608 (3), 1.62 (1) and 1.59 (2) for $\lambda = 0.01$, 0.05, 0.15, 0.30 and 0.50, respectively. This may be compared to the continuum result given in [26].

$$m_\phi = 2.642\,944\,662\,\tau_\phi^{5/12} \tag{3.6}$$

where m_ϕ is defined to be the lowest gap of the Hamiltonian (1.4). So we see no simple relation between the perturbation parameter τ_ϕ of (1.4) and the h, λ of (1.7).

3.2. Scaling of the bulk energy

Next we consider the bulk contribution to the energy levels. In the continuum theory, moving off-criticality, its change for $\tau_\phi \to 0$ is expected to have the scaling form [55]

$$E_i - E_{\text{bulk}}(\tau_\phi = 0) = -\kappa\mu^2 i + O(R^{-1}). \tag{3.7}$$

The coefficient κ has been computed in [26] from the thermodynamic Bethe ansatz on a strip of width R to be

$$\kappa = \frac{\sqrt{3}}{12}. \tag{3.8}$$

We want to check the behaviour (3.7) and the magnitude (3.8) of κ, on our chain. We choose to work at fixed λ and write for the eigenvalues of (1.7):

$$E_i(\lambda, \tau_v) = -(a_0(\lambda, \tau_v = 0) + \Delta a_0(\lambda, \tau_v))N + O(N^{-1}). \tag{3.9}$$

Since (3.7) refers to the conformally normalized H_ϕ of (1.4), (3.8) translates to

$$\lim_{\tau_v \to 0} \frac{\Delta a_0 \xi}{m^2} = \frac{\sqrt{3}}{12} \tag{3.10}$$

and, since $m \sim \tau_v^{5/12}$ for small τ_v, there we expect

$$\Delta a_0 \sim \tau_v^{5/6}. \tag{3.11}$$

In table 3 we list our results for the ratio $\Delta a_0 \xi / m^2$ for several values of τ_v. These show a clear tendency to converge towards $\sqrt{3}/12 = 0.1443$ but, even for the smallest values of τ_v which we can reach numerically, the results are still off this value by 15–25%. We can trace this discrepancy to the fact that the power law $\Delta a_0 \sim \tau_v^{5/6}$ is not well satisfied even for τ_v of the order of 0.001. Table 3 contains a few values for the effective exponent η defined through

$$\Delta a_0 \sim \tau_v^{\eta} \tag{3.12}$$

as measured from the curvature of the curve $\Delta a_0(\tau_v)$. In contrast to this, at such small values of τ_v, the power law for m, (4.2), is already well satisfied. We define an effective mass gap exponent ν by

$$m \sim \tau_v^{\nu} \tag{3.13}$$

and list a few values for ν in the last columns of table 3.

3.3. Check of the free particle energy–momentum relation

In the massive region $|h| < h_c(\lambda)$, the first excited level of the Hamiltonian (1.7) is expected to correspond to the single free particle state with the relativistic energy–momentum relation

$$\Delta E(P) = \sqrt{m^2 + P^2} \tag{3.14}$$

where for a periodic chain of length N,

$$P = 2 \sin(k\pi / N) \tag{3.15}$$

Table 3. Bulk scaling coefficient $\Delta a_0 \xi / m^2$ for various values of λ and small off-criticality τ_v. η and σ are the effective exponents for the off-criticality variation of the bulk term Δa_0, defined in (3.12), and the mass gap, (3.13), respectively

	$\Delta a_0 \xi / m^2$					η		σ	
τ_v	$\lambda = 0.01$	0.05	0.15	0.30	0.50	0.01	0.15	0.01	0.15
0.0001	0.124		0.131			0.806	0.811		
0.0002	0.121		0.127			0.803	0.805	0.418	0.42
0.0005	0.117		0.122			0.797	0.798	0.416	0.413
0.001	0.114	0.118	0.119	0.119	0.115	0.791	0.793	0.414	0.415
0.002	0.110	0.115	0.116	0.116	0.111	0.784	0.787	0.413	0.412
0.005	0.105	0.110	0.112	0.111	0.108	0.773	0.780	0.410	0.415

with $k=0,\ldots,N-1$. On the massive line of the thermally perturbed Ising model ($h=0, \lambda<1$) we know that the gap $\Delta E^{\text{Ising}}(k)$ between the lowest momentum k state of the $Q=1$ sector and the ground state E_g is given by [51–54]:

$$\Delta E^{\text{Ising}}(k)=\Lambda(2k)+E_a-E_g \tag{3.16}$$

where

$$E_a-E_g=-\frac{1}{2}\left(\sum_{k=0,2,4,}^{2N-2}\Lambda(k)-\sum_{k=1,3,5,}^{2N-1}\Lambda(k)\right) \tag{3.17}$$

and

$$\Lambda(k)=\sqrt{(1-\lambda)^2+4\lambda\sin^2(k\pi/2N)}. \tag{3.18}$$

For $\lambda<1$, E_a-E_g vanishes exponentially with N [52]. So, for $(1-\lambda)N\gg 1$ we get

$$\frac{\Delta E^{\text{Ising}}(k)}{\sqrt{\lambda}}=\sqrt{\frac{(1-\lambda)^2}{\lambda}+P^2} \tag{3.19}$$

which shows that for $h=0$ we have to use the normalized $H/\xi(\lambda, h)$ with $\xi(\lambda, h=0)=\sqrt{\lambda}$ in order to obtain the energy-momentum relation (3.14), (3 15).

On the $c=-\frac{22}{5}$ curve we found that for $\lambda\geq 0.1$ the conformal normalization is $\xi(\lambda, h_c)\approx\lambda^{5/12}$. Since $\lambda^{5/12}$ and $\sqrt{\lambda}$ do not differ much, except for small λ, for $\lambda\geq 0.1$, $\xi(\lambda, h)$ will have only a moderate h dependence.

We have tried to determine ξ at various points in the massive region by calculating

$$\xi^2(\lambda, h)=\frac{(\Delta E(0))^2-(\Delta E(P))^2}{P^2} \tag{3.20}$$

for $P^2=1, 2, 3, 4$, i.e. $N/k=6, 4, 3, 2$ Our results, given in table 4, show that for h close to h_c the relation (3.14), (3.15) is appreciably violated, so that no precise value for $\xi(\lambda, h)$ can be obtained. This is to be expected, since the momentum distribution of finite-N levels in the conformal spectrum does not follow the simple law $E=2\sin(k\pi/N)$. Anyway, table 4 gives an idea about how strongly the normalization of the chain Hamiltonian has to vary if we go off-critical.

3.4. Calculation of the phaseshift

The second, third and higher excited levels of the Hamiltonian in the massive region correspond to two- and multiparticle scattering states. Lüscher [56] has pointed out that from the N dependence of the two-particle levels for zero total momentum at fixed off-criticality τ, one can deduce the two particle S-matrix (see also [57, 61]). The application of this method to our case is particularly simple, since the massive theory in our off-critical region contains only one single type of neutral particle.

If there were no scattering, a two-particle eigenstate of the Hamiltonian would have the energy (with respect to the vacuum)

$$\Delta E_{a_1,a_2}(N)=\sqrt{m_1^2+P_1^2}+\sqrt{m_2^2+P_2^2} \tag{3.21}$$

where m_1, m_2 are the masses of the particles, and P_1, P_2 their momenta. On a chain of length N with a periodic BC, if the particles are bosons, P_1 and P_2 take the discrete values

$$P_i=2\sin(a_i\pi/2N) \qquad a_i=0, 2, 4,\ldots \qquad i=1, 2. \tag{3.22}$$

Table 4. Squared normalization factor ξ^2 as defined in (3.20). At $h = h_c$ from table 1 we get $\xi^2 = 0.0276$, 0.085, 0.1927 and 0.520, for $\lambda = 0.01$, 0.05, 0.15 and 0.50, respectively

			$\lambda = 0.01$			
P^2	$h = 0.50$	0.75	0.85	0.905 479	0.910 479	0.913 47
4	0.011 5470	0.015 117	0.018 964	0.023 048	0.023 203	0.022 85
3	0.011 5473	0.015 123	0.019 009	0.023 473	0.023 825	0.023 67
2	0.011 5477	0.015 129	0.019 051	0.023 896	0.024 474	0.024 60
1	0.011 5480	0.015 134	0.019 093	0.024 32	0.025 12	0.025 6
			$\lambda = 0.05$			
P^2	$h = 0.45$	0.70	0.75	0.757 43	0.760 43	0.761 43
4	0.055 977	0.069 447	0.072 25	0.070 96	0.069 06	0.067 67
3	0.056 009	0.070 042	0.074 12	0.073 33	0.071 70	0.070 12
2	0.056 040	0.070 613	0.076 12	0.076 11	0.074 74	0.073 14
1	0.056 070	0.071 19	0.078 2	0.079 16	0.079 1	0.078 3
			$\lambda = 0.15$			
P^2	$h = 0.20$	0.40	0.50	0.525	0.535	0.537 5
4	0.153 011	0.162 737	0.168 24	0.165 95	0.160 62	0.156 5
3	0.153 111	0.163 553	0.171 04	0.170 24	0.165 78	0.161
2	0.153 204	0.164 326	0.173 90	0.175 06	0.172 21	0.166
1	0.153 290	0.165 07	0.176 8	0.180	0.178	0.176
			$\lambda = 0.50$			
P^2	$h = 0.05$	0.106 2	0.136 2	0.146 2	0.151 2	0.155 2
4	0.499 350	0.494 99	0.485 72	0.477 7	0.469 9	0.453 8
3	0.499 822	0.497 50	0.490 66	0.482 7	0.474 0	0.455 4
2	0.500 33	0.499 89	0.495 0	0.489	0.480	0.462 9
1	0.500	0.502	0.504	0.503	0.502	0.50

In our case $m_1 = m_2 \equiv m$ and, considering only states of zero total momentum, we have $P_1 = -P_2$, so that $a_1 = a_2 \equiv a$ and

$$\Delta E_{a,a}(N) = 2\sqrt{m^2 + P_1^2}. \tag{3.23}$$

As shown by Lüscher, in the presence of an interaction described by the elastic S-matrix $S = \exp(2i\delta)$, a is no longer an even integer, but is modified to

$$a = 2n + 2\delta/\pi \qquad n = 0, 1, 2, \ldots. \tag{3.24}$$

The phaseshift δ is normalized conventionally to $\delta = \pi/2$ for $P_1 = P_2 = 0$.

Let us first apply (3.23) and (3.24) to the thermally perturbed Ising model which describes our case $h = 0$. There are $[N/2]$ two-particle levels with zero momentum in the $Q = 0$ sector. With respect to the ground state these have the energies

$$\Delta E_n^{\text{Ising, 2-particle}} = 2\Lambda(2n+1) \qquad n = 0, 1, \ldots, \left[\frac{N}{2}\right] - 1 \tag{3.25}$$

where Λ has been defined in (3.18). Normalizing the energies by $\sqrt{\lambda}$, as in (3.19), we see that this fits with (3.23) and (3.24) if $\delta = \pi/2$, independent of λ. This is the well-known Köberle-Swieca result [36] for the 'Ising field theory' [58–60].

Now we consider the off-criticality region of the $c = -\frac{22}{5}$ model. Its S-matrix (1.3) is equivalent to the phaseshift

$$\delta = \pi - \sin^{-1}\left\{\left[1+\frac{16}{3}\left(\frac{P_1}{m}\right)^2\left(1+\left(\frac{P_1}{m}\right)^2\right)\right]^{-1/2}\right\}. \tag{3.26}$$

In the non-relativistic limit $P_1 \ll m$ this reduces to

$$\delta = \frac{\pi}{2} + \frac{4}{\sqrt{3}}\frac{P_1}{m}\left[1-\frac{23}{18}\left(\frac{P_1}{m}\right)^2+\ldots\right]. \tag{3.27}$$

In order to calculate δ from our data for the gaps, we have used the two lowest two-particle levels corresponding to $n = 0, 1$, which are the second and third excited levels for zero-chain momentum of our Hamiltonian. We proceed as follows. We first choose a fixed value of λ. Then we consider a set of eight off-critical values of h which converge towards $h_c(\lambda)$. For these values of (h, λ) we use (3.23) to translate the gaps for each N into values of P_1/m. Then from (3.22) and (3.24) we get δ as

$$\delta = \frac{\pi}{2} - n\pi + N\sin^{-1}\left(\frac{P_1}{m}\frac{m}{2\xi}\right) \qquad n = 0, 1. \tag{3.28}$$

The factor ξ appears because of the requirement to normalize $\Delta E_{(a,a)}$ such that for the single particle gap the momentum dispersion relation (3.14), (3.15) is valid.

At each fixed (λ, h) the factor $m/2\xi$ is constant and we can draw a curve connecting the results for δ as a function of P_1/m by using various chain lengths N. Figures 4

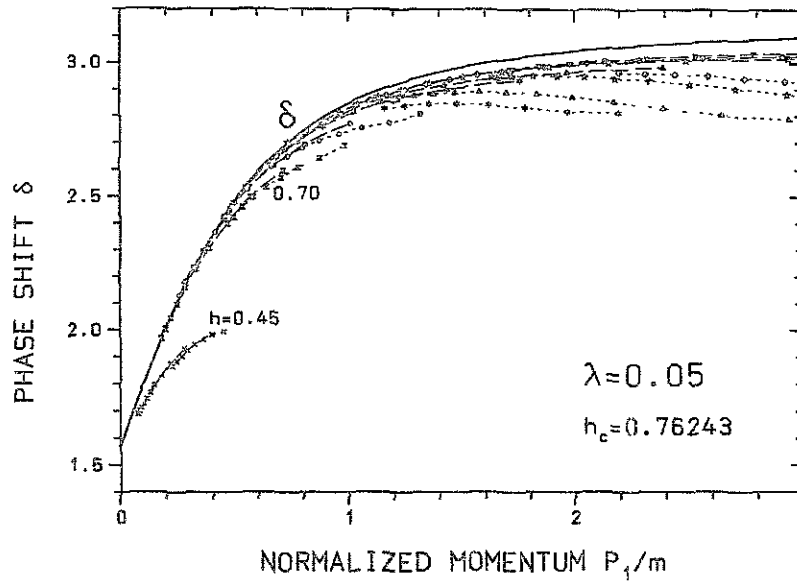

Figure 4. Full curves: phase shift δ as obtained from the minimal S-matrix (3.26), together with our finite-size approximations from the two lowest two-particle gaps $E_2 - E_0$ (long-broken curves) and $E_3 - E_0$ (short-broken curves), all at fixed $\lambda = 0.05$. ▽, ◇, ☆, △, +, ○, ⧖, × correspond to $h = 0.76193$, 0.76143, 0.76043, 0.75743, 0.75243, 0.73, 0.70, 0.45, respectively. The left-most points on each dashed curve correspond to the highest N-values. The critical value is $h_c = 0.76243$.

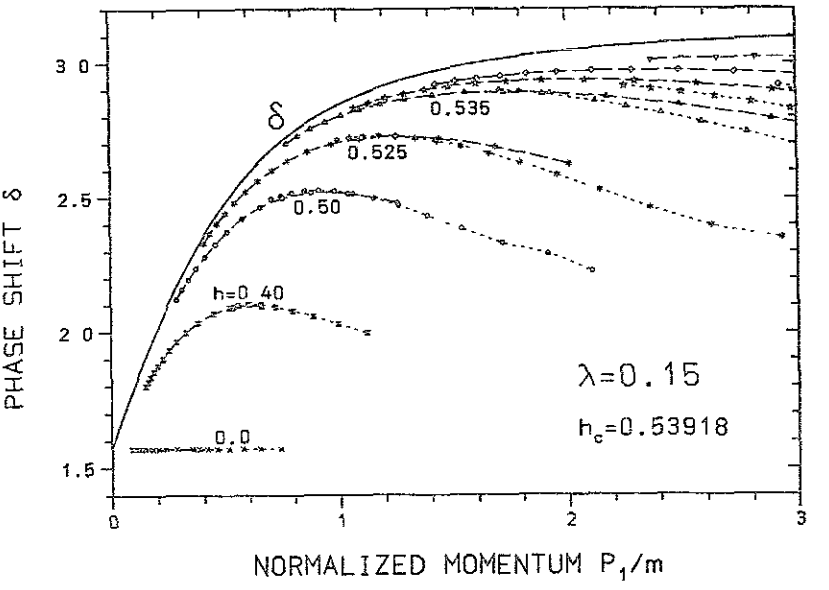

Figure 5. Same full curve for δ as in figure 4, together with our finite-size approximations at fixed $\lambda = 0.15$. Long-broken and short-broken curves as in figure 4 ∇, $\diamond$, $\star$, $\triangle$, $*$, $\circ$, $\boxtimes$, $\times$ correspond to $h = 0\ 5388$, $0\ 538$, $0\ 537$, $0\ 535$, $0\ 525$, $0\ 50$, $0\ 40$, $0\ 00$, respectively The critical value is $h_c = 0.539\ 177$ The left-most points on each curve are for $N = 19$ sites, then N decreases moving right along the curves.

and 5 show our curves. We see that at their left-most (large-N) wings these curves closely approach the curve for δ obtained from (3.26). Taking into account a variation of the normalization factor ξ with h as estimated from table 7 considerably improves the convergence and makes it useful to include quite large values of $h_c - h$. For large P_1/m we approach the conformal limit So, as noted recently by Lässig and Martins [61], on their right wings the curves are controlled by the conformal spectrum, which in our case means that they have to converge to $\delta = \pi$. Finally, observe in figure 5 the Ising value $\delta = \pi/2$ appearing for $h = 0$.

3.5. Scaling functions

In [26] the scaling functions $\mathcal{F}_i$ of the lowest energy levels of the continuum theory, defined in (1.5), have been calculated, using the truncated conformal Hilbert space method. Here we compare these results to the behaviour of our spin chain Hamiltonian (1.7).

It is useful, instead of the functions $\mathcal{F}_i$, to introduce functions $F_i(\mu, h)$ which have the leading large-μ behaviour extracted. Keeping λ fixed, we define

$$F_0(\mu, h) = -(E_0(N, h) - E_{\text{bulk}}(h))/m \tag{3.29}$$

$$F_i(\mu, h) = (E_i(N, h) - E_0(N, h) - m_i)/m \qquad i = 1, 2, 3 \tag{3.30}$$

where $E_0, \ldots, E_3$ are the four lowest zero-momentum eigenvalues of H, and

$$m_1 = m \qquad m_2 = m_3 = 2m. \tag{3.31}$$

Here m and E_{bulk} are the mass gap and the bulk energy of the infinite system, calculated at each fixed λ and h by extrapolation to $N \to \infty$. We denote the corresponding scaling functions by $F_i(\mu)$:

$$\lim_{\substack{h \to h_c \\ \mu \text{ fixed}}} F_i(\mu, h) = F_i(\mu) \qquad i = 0, \ldots, 3. \tag{3.32}$$

Both the low-μ and the large-μ behaviour of the $F_i(\mu)$ are known from different sources, as described below.

The small-μ limit of the $F_i(\mu)$ is dictated by conformal invariance to be

$$\lim_{\mu \to 0} F_i(\mu) = 4\pi c_i / \mu \tag{3.33}$$

with

$$c_0 = \tfrac{1}{30} \qquad c_1 = \tfrac{2}{5} \qquad c_2 = 1 \qquad c_3 = 2. \tag{3.34}$$

The explicit form of the large-μ limit of $F_0(\mu)$ has been obtained by Zamolodchikov from the thermodynamic Bethe ansatz [26]:

$$\lim_{\mu \to \infty} F_0(\mu) = K_0(\mu)/\pi \to (2\pi\mu)^{-1/2} \, \mathrm{e}^{-\mu} \tag{3.35}$$

where K_0 is a modified Bessel function. The large-μ behaviour of F_1 has been given in Yurov and Zamolodchikov [25] (the corrections to their result have been estimated recently by Klassen and Melzer [62]):

$$\lim_{\mu \to \infty} F_1(\mu) = 3 \, \mathrm{e}^{-(\sqrt{3}/2)\mu} - \int_{-\infty}^{\infty} \frac{\mathrm{d}\theta}{2\pi} \mathrm{e}^{-\mu \cosh \theta} \left(\frac{\sqrt{3} \cosh \theta}{\cosh \theta - \sqrt{3}/2} \right). \tag{3.36}$$

For the interesting range $6 < \mu < 10$ the right-hand side of (3.36) is well approximated by

$$F_1(\mu) \approx 1.93 \exp(-0.84\mu). \tag{3.37}$$

The large-μ behaviour of $F_2(\mu)$ and $F_3(\mu)$ is related to the small-P_1 behaviour of the phaseshift. Performing a non-relativistic expansion of (3.23) we get

$$F_2 = P_1^2/m^2 + \ldots = (4/m^2) \sin^2(\delta/N) + \ldots \tag{3.38}$$

which, because of (3.27), leads to

$$\lim_{\mu \to \infty} F_2(\mu) = \pi^2/\mu^2 \tag{3.39}$$

and analogously, using (3.24) with $n = 1$,

$$\lim_{\mu \to \infty} F_3(\mu) = 9\pi^2/\mu^2 \tag{3.40}$$

One might improve on (3.39) and (3.40) by taking into account the 'effective range' term of (3.27).

In order to present our results for finite chains, we first fix λ at $\lambda = 0.15$, so that we are on a vertical line in figure 1. We then consider six values of h converging from below to the critical point h_c. Since the power law for the mass m, (3.2), is not valid for larger values of $\tau_v = h_c - h$ (see figure 3), we do not define the scaling variable by $N\tau_v^{5/12}$ in analogy to (1.6), but instead we calculate the actual mass gap m at each (λ, h) in the limit $N \to \infty$ and then take as our scaling variable

$$\mu_m = Nm/\xi. \tag{3.41}$$

Now, similarly to our calculation of the phaseshift, for each of the six values of h we then draw curves of the functions F_i against μ_m, as they are obtained by varying N only.

Figure 6 shows these four functions on a double logarithmic scale for the particular value $\lambda = 0.15$. We have added full lines on the small-μ_m side indicating the low-μ_m behaviour expected from conformal invariance equations (3.33), and long-broken lines on the large-μ_m side, indicating the expected large-μ_m behaviour, (3.35), (3.36), (3.39) and (3.40).

The data show that for small values of N (the left-most points of each curve correspond to the smallest values of N), the F_i still show a h dependence. So there scaling is not yet perfect, but a limiting curve clearly emerges. We also see that the two-particle functions F_2, F_3 have not reached their asymptotic μ_m^{-2} power behaviour at $\mu_m = 12$, in contrast to the exponentially behaving F_0 and F_1.

Since we shall give the information contained in the F_i in a different form for more values of λ below, we only mention that, varying λ in the large range 0.01–0.5, the

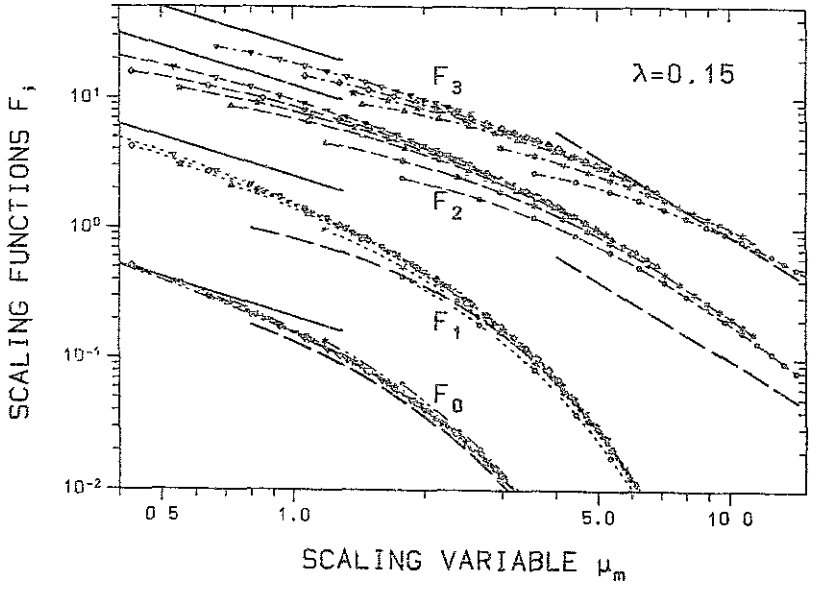

Figure 6. Scaling functions $F_i(\mu_m, \lambda)$ for the ground state ($i = 0$) and the three lowest gaps ($i = 1, 2, 3$), as defined in (3.29) and (3.30), for $\lambda = 0.15$ and six values of h each ∇, $\diamond$, $\star$, $\triangle$, $+$, $\circ$ correspond to $h = 0.5388$, 0.538, 0.537, 0.535, 0.525, 0.50, respectively. The curves connect the values obtained at fixed h for different values of N, starting from the left to right with $N = 2, 3,$ for the two lowest gap and with $N = 5, 6, \ldots$ for the third gap. The full curves on the left show the low-μ limiting behaviour (3.33), the long-broken curves on the right show the large-μ limiting behaviour, (3.35), (3.37), (3.39) and (3.40).

limiting curves for the F_i show no λ dependence. For $\lambda > 0.5$ just the convergence becomes poor.

In order to make the test of the λ independence more sensitive, and to present our results in an easily reproducible way, we parametrize the functions $F_i(\mu_m, h)$ such that the known small- and large-μ behaviour in the scaling limit is built in, and only the deviations due to a lack of scaling and due to eventual poor interpolation between small- and large-μ regions will be displayed. For simplicity, for F_0 and F_1 we chose to interpolate between the small- and large-μ regions by $\tan^{-1}$ functions, and to define new functions f_0 and f_1 by

$$F_0(\mu_m, h) = \frac{e^{-\mu_m}}{(4\mu_m \tan^{-1}(225\ \mu_m/4\pi^2))^{1/2}} f_0(\mu_m, h) \tag{3.42}$$

$$F_1(\mu_m, h) = \frac{\pi\, e^{-0.84\mu_m}}{\tan^{-1}(5\mu_m/4)} f_1(\mu_m, h). \tag{3.43}$$

If the scaling limit is reached and if the interpolation ansatz makes sense, we should get $f_0 \approx f_1 \approx 1$ for all μ_m.

Before discussing our numerical results for the f_i, we also consider the next two zero-momentum levels, which are the two-particle gap functions F_2 and F_3. These need a slightly different treatment, because we have seen in figure 6 that the asymptotic μ_m^{-2} behaviour is not yet obtained for the values $\mu_m \leq 12$, which we can reach with our chains of only up to $N = 19$ sites. However, in the intermediate range $2 \geq \mu_m \geq 12$ both

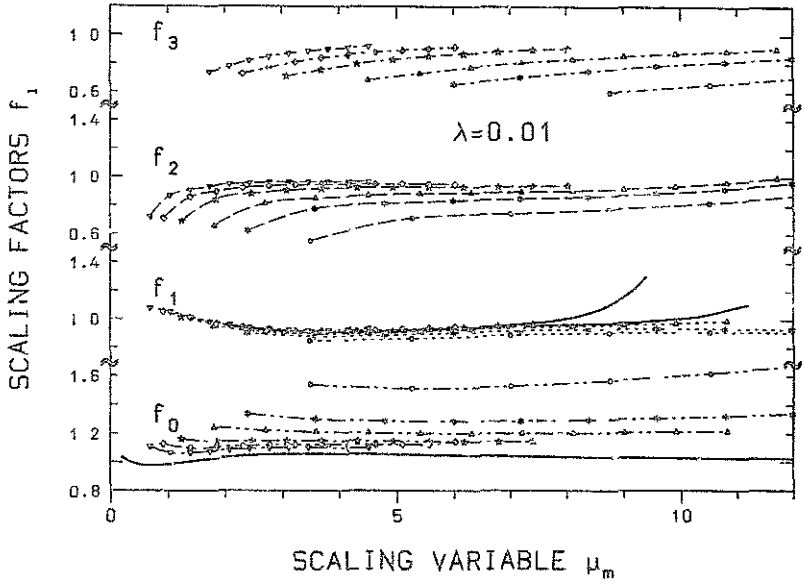

Figure 7. Scaling functions $f_i(\mu_m, h)$ as defined in (3.42)–(3.45), for $\lambda = 0.01$ ∇, $\diamond$, $\star$, $\triangle$, $+$, $\circ$ correspond to $h = 0.914\,979$, $0.914\,479$, $0.913\,479$, $0.910\,479$, $0.905\,479$, 0.89, respectively. The critical value is $h_c = 0.915\,479$. The left-most points of the dashed curves are from $N = 2$ sites, then on the curves N increases towards the right. Full lines: curves for f_0 and f_1 calculated from the tables of [25]. The upper branch in the full curve for f_1 is the fourth-level truncation result, the lower from fifth-level truncation.

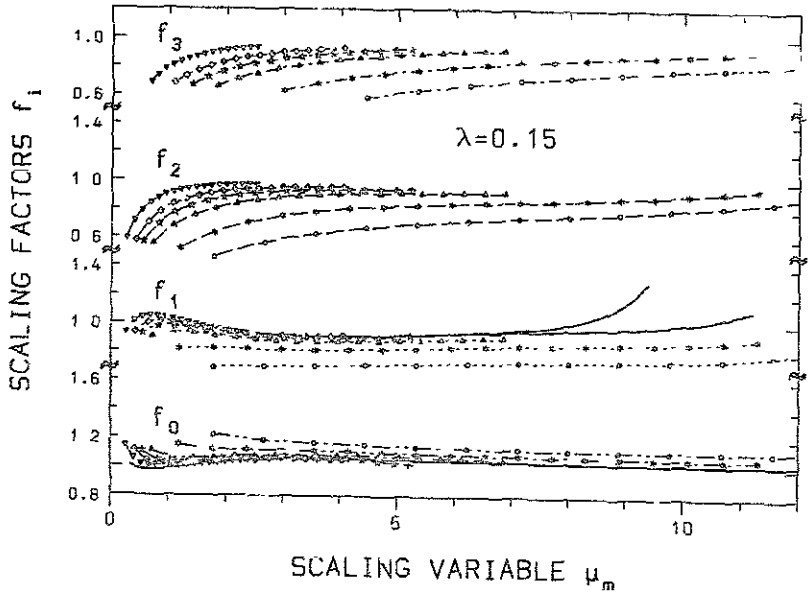

Figure 8. Scaling functions $f_i(\mu_m, h)$ as in figure 7, but for $\lambda = 0.15$. The symbols on the curves correspond to the same values of h as in figure 4. Full lines as before.

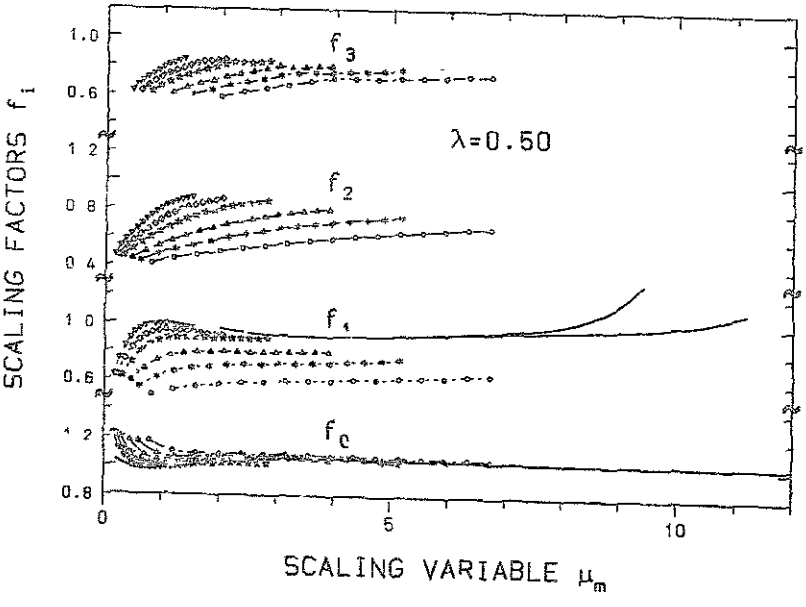

Figure 9. Scaling functions $f_i(\mu_m, h)$ as in figure 7, but for $\lambda = 0.50$. ▽, ◇, ☆, △, *, ○ correspond to $h = 0.1557$, 0.1552, 0.1542, 0.1512, 0.1462, 0.1362, respectively. Full lines as in figure 7.

F_2 and F_3 are quite good exponentials. So it makes sense to define f_2 and f_3 by the ansatz

$$F_2(\mu_m, h) = 4\pi\mu_m^{-1}\, e^{-0.17\mu_m} f_2(\mu_m, h) \tag{3.44}$$

$$F_3(\mu_m, h) = 8\pi\mu_m^{-1}\, e^{-0.08\mu_m} f_3(\mu_m, h) \tag{3.45}$$

which for $f_2 \approx f_3 \approx 1$ have the correct low-μ conformal limit and simulate well the intermediate trend.

Figures 7–9 show our results for the $f_i(\mu_m, h)$ $(i = 0, 1, 2, 3)$. Each broken curve refers to a fixed value of h and connects our results for the $f_i(\mu_m, h)$ obtained from different N (which at fixed h correspond to different values of μ_m). The left-most points on the curves of f_0, f_1 and f_2 are from $N = 2$ sites only ($N = 5$ sites for f_3) then, moving on the curves to the right, the symbols mark the increase of N in steps of unity.

As h approaches h_c, a limiting curve very close to $f_i \equiv 1$ is seen to emerge in all cases. Comparing figures 7–9, no change of the limiting curves with λ is visible. So our calculations show that the scaling functions $F_i(\mu)$ are universal along the $c = -\frac{22}{5}$ critical curve from $\lambda = 0.01$ to 0.5. Numerically this is obtained in a quite non-trivial way, since ξ and m behave very differently for small and large values of λ.

Drawn as full lines, in figures 7–9 we also show the results for f_0 and f_1 of the truncated Hilbert space and the thermodynamic Bethe ansatz calculations of Yurov and Zamolodchikov [25, 26]. For this we have translated the data for $E_0 + a_0 N$ and $E_1 + a_0 N - m$ as functions of μ_ϕ, which are given in the tables of [25], into our f_0 and f_1. We see that there is good agreement of our Ising chain results with the continuum theory data.

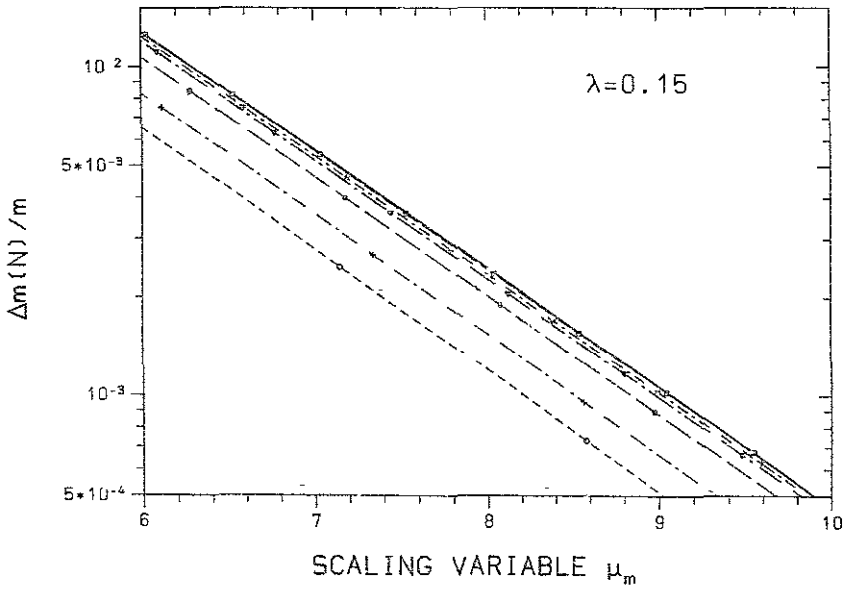

Figure 10. Full line large-μ approximation of the mass gap function F_1 (3.30), together with our finite-chain results for $h = 0.40$, 0.45, 0.50, 0.52, 0.525, 0.53, represented by the symbols ◇, +, ○, ▽, ×, □, respectively. The critical value is $h_c = 0.539\,177$. For example, the small squares shown on the curve for $h = 0.40$ are from the $N = 5$ and 6 sites, the asterisks for $h = 0.525$ are from the $N = 11$–16 sites.

Finally, in figure 10, in a kind of 'blow-up' from figure 8, we test the validity of the large-μ estimate (3.36) for the mass gap scaling function $F_1(\mu)$. We take $\lambda = 0.15$. The various broken curves in figure 10 show our data for $F_1(\mu_m, h)$ at various values of h converging to the critical value $h_c = 0.539\,177$, together with a full line representing the right-hand side of (3.36). The slope is perfectly reproduced, and the agreement with the absolute value leaves very little space for higher corrections

4. Boundary condition dependence

In the above sections we always used periodic boundary conditions $\sigma^x_{N+1} = \sigma^x_1$. In this section we shall now show that the position of the Yang-Lee singularity and the structure of the conformal spectrum depends in a quite peculiar way on the boundary condition. We shall consider $\sigma^x_{N+1} = a\sigma^x_1$. (1.8), where we shall keep a real, in order not to spoil the reality of the coefficients of the characteristic polynomial of H.

We have studied the range $-3 < a < +\infty$, which includes the periodic ($a = 1$) and free ($a = 0$) BC cases. The case $0 < a < 1$ may be interpreted as having a defect on the chain [63–65].

4.1. Boundary dependence of the position of the Yang-Lee singularity

In figure 11 we show the position of the lowest-level crossings (Yang-Lee square root branch points) for finite chains of $N = 5, 7, \ldots, 15$ sites in the plane of the boundary parameter a and the imaginary field h. The inverse temperature λ is chosen to be fixed at $\lambda = 0.15$, so that the critical imaginary field is $h_c = 0.539\,177$. We see that only for

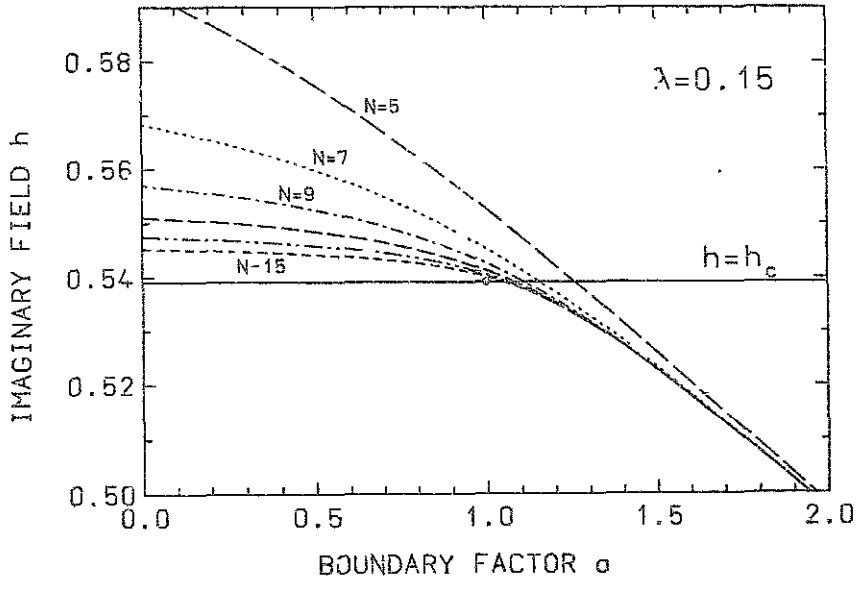

Figure 11. Curves showing the location of the lowest-level crossing (Yang-Lee square root branch points) for finite chains with $N = 5, 7, 9, 11, 13$, and 15 sites in the (h, a) plane. The horizontal full line marks the $c = -\frac{22}{5}$ critical value $h_c = 0.539\,177$

$a \leqslant 1$ is the Yang–Lee singularity on the critical line for $N \to \infty$. Surprisingly, for $a > 1$ the Yang–Lee singularity moves to the massive region $h < h_c$ and the convergence to the limiting curve with increasing N becomes very fast (probably exponential, controlled by the correlation length), in contrast to the power law $N^{-2.4}$, (2.6), which we find for $a \leqslant 1$.

In order to give an idea what happens for a outside the range of figure 11, we mention that for *large* a the Yang–Lee singularity position $h_{YL}(a)$ (always for λ fixed) follows the law $h_{YL} \sim a^{-1}$. At $\lambda = 0.15$ we find $h_{YL} = 2.7707/a$ for $a \to \infty$. Still for $\lambda = 0.15$, we get $h_{YL} = 0.3$ and 0.1 at $a = 6.929\,63$ and 26.89, respectively.

The fact that for a fixed value of h and λ in the massive region, the ground state can be changed from singly (for $a \leqslant 1$) to doubly degenerate at the Yang–Lee singularity (which occurs for $a > 1$) just by changing a boundary term requires further investigation. We have checked that on the Yang–Lee curve at $a > 1$ the next energy level follows the degenerate ground state precisely at the distance of $m(h, \lambda)$, where m is the mass gap as determined for a periodic BC.

For $a < 1$ the power law of the approach to criticality, (2.6), seems to remain unchanged even to very low a. However, the convergence becomes less fast, which results in an increase of the coefficient B. For example, in the Ising case $\lambda = 1$ we find

$$B(\lambda = 1, a = 0) = 2.004\,(6) \qquad B(\lambda = 1, a = -1) = 4.0707\,(2). \tag{4.1}$$

4.2. The Yang–Lee singularity as a branch point in the boundary factor a

In the following we take λ and h to be fixed on the critical $c = -\frac{22}{5}$ curve of the infinite system ($h = h_c$ in figure 11).

As we have just seen in figure 11, for $a \leqslant 1$ the square root branch points approach the line $h = h_c$ from *above* with increasing N (at least for the lowest levels, see the footnote to (2.2)) so that there the finite-size spectra are real. For $a > 1$, however, for sufficiently large N the spectra are complex at $h = h_c$, because we are beyond the Yang–Lee singularity. In table 5 we give the branch point positions $a_{YL}(\lambda, N)$ for two fixed values of (λ, h) on the critical curve.

We fit the sequence of the $a_{YL}(\lambda, N)$ at fixed λ to the form

$$a_{YL}(\lambda, N) = 1 + D(\lambda) N^{-\rho} + \ldots \tag{4.2}$$

and write the lowest gap ΔE for small $a_{YL}(\lambda, N) - a$ in analogy to (2.4) and (2.5) as

$$\Delta E(\lambda, h_c(\lambda), a, N) = C(\lambda, N)\sqrt{a_{YL}(\lambda, N) - a} + \ldots \tag{4.3}$$

with

$$C(\lambda, N) = C(\lambda) N^{-\gamma} + \ldots . \tag{4.4}$$

Conformal invariance at $a = 1$, (2.8), gives $\gamma + \rho/2 = 1$ and $C(\lambda)\sqrt{D(\lambda)} = 2\pi x \xi(\lambda)$. Introducing the variable μ_a by

$$\mu_a = \frac{(1-a)N^{\rho}}{D(\lambda)} \tag{4.5}$$

for small $|1 - a|$ we can write

$$\Delta E(\lambda, h_c(\lambda), a, N) = \frac{2\pi x \xi}{N}\sqrt{1 + \mu_a} + \ldots . \tag{4.6}$$

Table 5. Lowest gap branch point position $a_c(N)$ in the boundary variable a for finite chains of length N, for two values of (λ, h) on the critical curve, together with exponents ρ and coefficient C, as defined in (4.2) and (4.3), respectively

	$\lambda = 0.05$, $h = 0.762\,43$			$\lambda = 0.15$, $h = 0.539\,18$		
N	$a_c(N)$	$\rho(N)$	$C(\lambda, N)$	$a_c(N)$	$\rho(N)$	$C(\lambda, N)$
3	1.438 170 0773	1 667 63	0 364 834	1 590 154 776	1 676 75	0 446 244
4	1.271 200 8638	1 569 87	0 356 717	1 364 312 837	1.574 48	0 446 615
5	1 191 053 2718	1 521 08	0 344 783	1 256 384 602	1 524 30	0 436 640
6	1.144 781 5 325	1.492 44	0 332 924	1 194 176 250	1 495 16	0 424 384
7	1 115 026 8607	1.473 89	0 322 03	1 154 205 495	1.476 46	0 412 168
8	1 094 476 9031	1 461 06	0 312 18	1 126 612 665	1 463 64	0 400 687
9	1 079 540 5904	1 451 76	0 303 35	1 106 563 494	1.454 44	0 390 112
10	1.068 258 99	1 444 80	0 295 4	1 091 423 314	1 447 63	0 380 43
11	1 059 477 9	1.439 40	0 288 1	1 079 540 810	1 442 48	0 371 58
12	1 052 476 2	1 435 27	0.281 7	1.070 246 764	1 438 53	0 363 45
13	1 046 781 1		0 275	1 062 606 54	1 435 50	0 355 99
14	1 042 072			1 056 288 39	1 433 17	0 349 09
15	1 038 1			1.050 988 94		0.342 68
∞	1.000 0 (1)	1 42 (6)		1 004 (5)	1.42 (1)	

Table 5 also contains the values for $C(\lambda, N)$ and finite-N approximants to ρ for two different values of λ. The values obtained for the exponents γ and ρ are not very precise. We can only state that $\rho \approx 1.4$.

4.3. Decoupling of the primary field $\phi_{(-1/5,-1/5)}$ for $a < 1$

If we take a to be smaller than 1, our data for the lowest gap change drastically. Consider the a-dependent expression

$$\mathscr{E}_1(\lambda, h_c, a) = \lim_{N\to\infty} \mathscr{E}_1(\lambda, h_c, N, a)$$

$$= \lim_{N\to\infty} \frac{N}{2\pi\xi(\lambda)} (E_1(\lambda, h_c, a, N) - E_0(\lambda, h_c, a, N)). \tag{4.7}$$

In contrast to our definition (2.2) in section 2, here it is useful to refer the scaled gaps $\mathscr{E}_i$ to the lowest level E_0, not to the vacuum E_{vac}. For a periodic BC, $a = 1$, we have $\mathscr{E}_1(\lambda, h_c, a) = \frac{2}{5}$, but table 6 shows that already at $a = 0.95$, for large N, the $\mathscr{E}_0(\lambda, h_c, a, N)$ tend to one and stay at one for all a down to the antiperiodic case $a = -1$ (and even further). Because, in the situation with a boundary, we have to define the surface exponents x_i^s by

$$\lim_{N\to\infty} \mathscr{E}_i(\lambda, h_c, a, N) = \tfrac{1}{2}x_i^s(a) \tag{4.8}$$

this means that for $a < 0.95$ we get $x_1^s \approx 2$ so that there is no longer the contribution of the primary field $\phi_{(-1/5,-1/5)}$ but only that of the unit operator, and now the ground state is the vacuum state. This is confirmed by the calculation of the effective central charge from the N^{-1} term of the ground state energy (see (2.3)). We estimate $\hat{c}$ from the large N-extrapolation of

$$\tfrac{1}{2}(N^2-1)N(E_0(N+1) - 2E_0(N) + E_0(N-1)) = -\frac{\hat{c}\pi\xi}{24} + \dots \tag{4.9}$$

Table 6. Scaled lowest gap, $\mathscr{E}_1$, as defined in (4.7) at the critical point $h_c(\lambda = 0.15) = 0.539\,18$, for the boundary condition a changing from periodic over free to antiperiodic. Since $\mathscr{E}_1(N \to \infty) = x_1^2/2$, we see that for $a \leq 0.95$ the data indicate $x_1^2 = 2$.

N	$a = 1.0$	0.95	0.90	0.75	0.50	0.00	−1.00
2	0.352 49	0.359 91	0.367 23	0.388 73	0.423 22	0.488 70	0.612 47
3	0.375 29	0.390 80	0.405 69	0.447 07	0.507 24	0.602 72	0.721 67
4	0.385 59	0.409 94	0.432 56	0.492 15	0.571 10	0.679 53	0.793 49
5	0.390 88	0.424 54	0.454 78	0.530 26	0.621 91	0.733 78	0.840 09
6	0.393 90	0.437 19	0.474 76	0.563 73	0.663 23	0.773 63	0.871 85
7	0.395 76	0.448 90	0.493 40	0.593 56	0.697 30	0.803 87	0.894 44
8	0.396 98	0.460 08	0.511 08	0.620 29	0.725 72	0.827 46	0.911 10
9	0.397 81	0.470 94	0.527 96	0.644 33	0.749 66	0.846 30	0.923 77
10	0.398 39	0.481 55	0.544 10	0.665 99	0.770 03	0.861 65	0.933 65
11	0.398 81	0.491 95	0.559 54	0.685 52	0.787 52	0.874 35	0.941 52
12	0.399 11	0.502 16	0.574 31	0.703 18	0.802 66	0.885 04	0.947 92
13	0.399 33	0.512 18	0.588 42	0.719 18	0.815 88	0.894 12	0.953 21
14	0.399 48	0.522 00	0.601 90	0.733 71	0.827 50	0.901 95	0.957 63
15	0.399 59	0.531 62	0.614 75	0.746 93	0.837 80	0.908 74	0.961 37
16	0.399 66	0.541 03	0.627 00	0.758 99	0.846 97	0.914 69	0.964 57
∞	0.399 9 (2)	0.98 (6)	0.93 (3)	0.99 (2)	1.01 (4)	1.00 (1)	0.997 (4)

In table 7 we give our results for $\hat{c}$ together with the first few low levels x_i^s, calculated from (4.9). We again see that for at least $a \leq 0.75$ the spectrum is that of the unit operator only, and that the effective central charge of the ground state is $\hat{c} = -\frac{22}{5}$ within the errors.

So, the Yang–Lee singularity for free BC gives rise to what may be called a 'simplest conformal system', since it contains only the unit operator and no non-trivial primary field. This situation is also encountered in the analysis of the xxz Heisenberg chain with a special BC: there the same spectrum with the same central charge $c = -\frac{22}{5}$ appears (see (2.38) and (2.39) of [66]).

While in the present case of the $c = -\frac{22}{5}$ critical line the spectrum changes quite abruptly when varying the boundary condition, for the Ising transition at $h = 0$ it is known [63, 64] that there the change is smooth (however, see also [65]).

Table 7. Effective central charge $\hat{c}$ and effective surface exponents x_i^s for the lowest levels of the Hamiltonian (1.7) for various boundary factors a. Observe that for the periodic BC we have $c_{\text{eff}} = \hat{c}/4$ and $\gamma_i = x_i^s/2$.

a	$\hat{c}$	x_i^s (parity +)	x_i^s (parity −)
1.00	+1.68 (4)	0.84 (2), 1.66 (1), 4.01 (1), 4.5 (1), 5.6 (1)	
0.90	−3.9 (8)	1.86 (6), 3.5 (9), 4.6 (8), 5.6 (6), 5.7 (5)	
0.75	−4.2 (5)	1.98 (4), 3.8 (2), 4.8 (7), 5.9 (5), 6.0 (2)	
0.50	−4.2 (4)	2.02 (8), 3.96 (7), 6.0 (2), 5.8 (3)	2.98 (6), 4.9 (4)
0.00	−4.42 (2)	2.00 (1), 4.01 (1), 5.9 (1), 5.94 (8)	2.99 (4), 5.05 (8)
−0.5	−4.46 (6)	2.00 (2), 3.99 (2), 6.0 (2), 6.1 (3)	3.02 (7), 5.05 (8)
−1.0	−4.38 (5)	1.994 (8), 4.00 (5), 6.05 (8), 6.00 (7)	3.00 (2)
−2.0	−4.40 (4)	2.00 (2), 4.00 (2), 5.8 (1), 6.1 (2)	
−3.0	−4.42 (6)	2.01 (4), 4.02 (1), 6.05 (8), 5.9 (3)	

5. Yang–Lee branch points in the antiferromagnetic region

Since for the Ising quantum chain without field ($h=0$) there is a correspondence of the spectrum [51-54] in the ferromagnetic region $\lambda>0$ and the spectrum in the antiferromagnetic region $\lambda<0$, the question arises whether there is a Yang–Lee branch point also for $\lambda<0$. We shall only consider the case of a homogeneous (non-staggered) field, i.e. as in all previous sections, we use (1.7), with h independent of the site position i.

Let us first give the ferromagnetic/antiferromagnetic interrelation at $h=0$ for the boundary conditions $a=+1, 0$ and -1:

The *sum* of the periodic and antiperiodic spectra is unchanged if we replace λ by $-\lambda$, but

(i) for an *odd* number of sites N the $a=1$-eigenvalues at a value λ appear for $-\lambda$ at $a=-1$;

(ii) for an *even* number of sites the eigenvalues remain in the same BC sector but, in the Z_2 odd sector, positive-parity eigenvalues at λ are equal to negative-parity eigenvalues at $-\lambda$. The Z_2 even eigenvalues do not change parity in going from λ to $-\lambda$.

For the free BC we have just the parity rule (ii), otherwise the spectra at $\pm\lambda$ are the same.

Now going to $h\neq 0$, our calculation of the spectra at $\lambda<0$ shows the following features:

In the periodic and free BC cases ($a=1$ and $a=0$) for an *even* number of sites, there is no crossing of the two lowest levels for negative λ and all h. Only the second and third levels meet with increasing h and form a complex conjugate pair. So, in this case the mass gap does not vanish

However, for *odd* N, the two lowest levels meet in the same way as in the region $0<\lambda<1$. The corresponding branch point positions $h_c(\lambda, N)$ are given in tables 8 and 9. For the periodic BC the limiting curve $h_c(\lambda)$ where the mass gap vanishes rises from $h_c=1$ at $\lambda=0$ to $h_c(\lambda)=2$ for large negative values of λ. In the free BC case instead, the curve $h_c(\lambda)$ falls towards $\lambda=-1$.

For the antiperiodic BC there is a meeting of the two lowest levels for both even and odd N. Both approach the same curve $h_c(\lambda)$ for $N\to\infty$, but from opposite directions. The branch point positions are listed in table 10. Note that in all three BC cases for odd N the convergence with N is from below, so that at $h_c(\lambda)$ the eigenvalues are still complex for finite N, only in the limit do they become real.

The absence of a crossing of the lowest levels in the cases of periodic and free BCs and even number of sites is due to the fact that in these two cases the ground state and first excited state have different parity (rule (ii) above) and therefore cannot merge to form a complex conjugate pair.

We have checked that points on the curve of vanishing mass gap for $-1<\lambda<0$ and antiperiodic BC show no conformal invariance†: at both $(\lambda, h)=(-0.2, 0.855\,315)$ and $(\lambda, h)=(-0.5, 0\,643\,65)$ for even N, the lowest gap vanishes exponentially with N and the second gap falls slower than N^{-1}.

The branch point positions $h_c(\lambda=-1, N)$ for the free BC approach zero proportional to $N^{-0.500(4)}$ (for odd N), whereas with the antiperiodic BC for odd and even N we find a power behaviour proportional to $N^{-0.88(1)}$ and $N^{-0.92(2)}$, respectively, in contrast to the behaviour at $\lambda=+1$, (2.15) (see also (4.1)).

† For an example of a conformal antiferromagnetic system, see the discussion of the spin-1-Zamolodchikov-Fateev quantum chain in [67] and references therein.

Table 8. Branch point positions $h_c(\lambda, N)$ for finite-size chains with antiperiodic boundary condition in the antiferromagnetic regime

N	$\lambda=-0.2$	$\lambda=-0.5$	$\lambda=-0.8$	$\lambda=-1.0$
2	1.000 000 0000	1.000 000 0000	1.000 000 0000	1.000 000 0000
3	0.830 910 8850	0.605 911 6903	0.399 745 3567	0.296 933 4269
4	0.877 316 1326	0.748 571 8089	0.646 545 0454	0.593 558 3969
5	0.847 425 9328	0.609 311 3800	0.329 643 4721	0.187 693 9808
6	0.859 604 6732	0.683 634 0863	0.523 291 8536	0.439 514 0762
7	0.853 526 9095	0.625 129 5591	0.311 249 9611	0.139 714 3161
8	0.856 141 7280	0.659 433 7921	0.457 702 9162	0.350 553 6898
9	0.854 960 7385	0.635 082 6338	0.308 404 3513	0.112 222 6797
10	0.855 470 1451	0.649 944 8628	0.418 772 0882	0.292 680 8429
11	0.855 248 9682	0.640 002 3821	0.311 274 0188	0.094 245 1200
12	0.855 343 5279	0.646 167 4487	0.394 106 6223	0.251 956 2272
13	0.855 303 1954	0.642 181 7577	0.316 056 6388	0.081 505 1554
14	0.855 320 2841	0.644 664 3869	0.377 832 3467	0.221 682 4065
15	0.855 313 0677	0.643 090 4280	0.321 086 9383	0.071 972 1804
∞ even	0.855 318 (4)	0.643 658 (1)	0.338 (2)	−0.01 (1)
∞ odd	0.855 315 (1)	0.643 652 (4)	0.348 (7)	0.001 (1)

Table 9. Branch point positions $h_c(\lambda, N)$ for finite-size chains with free boundary condition in the antiferromagnetic regime

N	$\lambda=-0.05$	$\lambda=-0.2$	$\lambda=-0.5$	$\lambda=-0.8$	$\lambda=-1.0$	$\lambda=-1.2$
3	1.043 3783	1.062 1489	0.971 2261	0.793 8649	0.660 2971	0.535 9957
5	1.061 4410	1.097 4663	0.991 9719	0.736 4234	0.526 3338	0.341 5795
7	1.071 4437	1.119 2031	1.014 2226	0.716 6184	0.450 1454	0.229 2334
9	1.077 7531	1.133 7119	1.032 9730	0.710 9850	0.399 5401	0.156 9392
11	1.082 0229	1.143 9100	1.048 1967	0.711 5326	0.362 8396	0.108 3354
13	1.085 0241	1.151 3104	1.060 5300	0.714 9221	0.334 6695	0.075 0446
15	1.087 1827	1.156 7823	1.070 5779	0.719 5927	0.312 1717	0.052 0607
∞	1.093 (1)	1.174 (2)	1.108 (2)	0.75 (2)	0.03 (5)	0.000 0 (1)

Table 10. Branch point positions $h_c(\lambda, N)$ for finite-size chains with periodic boundary condition in the antiferromagnetic regime

N	$\lambda=-0.02$	$\lambda=-0.2$	$\lambda=-0.4$	$\lambda=-1.0$	$\lambda=-10.0$
3	1.065 563 255	1.282 906 280	1.421 570 852	1.659 418 709	1.989 094 316
5	1.072 775 173	1.312 597 206	1.462 838 684	1.709 136 247	1.992 645 633
7	1.075 104 902	1.321 435 552	1.474 120 808	1.719 100 226	1.992 670 872
9	1.076 161 250	1.325 141 191	1.478 436 600	1.721 754 919	1.992 671 07
11	1.076 734 385	1.327 004 480	1.480 402 994	1.722 561 121	1.992 671 08
13	1.077 082 071	1.328 052 345	1.481 397 795	1.722 823 515	
∞	1.078 1 (1)	1.330 3 (1)	1.482 9 (1)	1.722 96 (7)	1.992 671 1 (1)

6. Conclusions

Calculating numerically the lowest-level crossings, we performed a precision determination of the $c=-\frac{22}{5}$ critical curve of the Ising quantum chain with an imaginary field h, defined by the Hamiltonian (1.7). This opens the possibility of studying the conformal and off-critical properties of the $c=-\frac{22}{5}$ theory using finite Ising quantum chains. We give the behaviour of the lowest gap in the vicinity of the corresponding square root branch point. The conformal normalization factor along the $c=-\frac{22}{5}$ line is calculated from the conformal spectrum.

Defining a scaling variable using the 'measured' actual mass gap (which only for small off-criticality follows the $\frac{5}{12}$ power law), the scaling functions are universal along the $c=-\frac{22}{5}$ curve and agree very well with the result of the truncated Hilbert space method of Yurov and Zamolodchikov [25] We find that the free energy–momentum relation (3.14) and (3.15), which is exact for $h=0$, is considerably violated if we approach the $c=-\frac{22}{5}$ line (see table 7).

The bulk scaling coefficient obtained from our calculation is compatible with the thermodynamic Bethe ansatz result of [26], although the bulk term approaches the expected $\frac{5}{6}$ power law only for very small off-criticality. The calculation of the S-matrix (or the corresponding phaseshift δ) by Lüscher's method is in excellent agreement with the minimal S-matrix of Cardy and Mussardo.

The boundary condition dependence of the spectrum is found to be quite peculiar: for free and antiperiodic BCs the conformal spectrum is produced by the tower of the unit primary field only, resulting in the 'simplest conformal spectrum' one can imagine. If the boundary factor $a>1$, for the parameter values $h=h_c(\lambda)$, i.e. on the conformal line, finite chains show a spectrum with complex conjugate pairs of eigenvalues. This is a result of the Yang–Lee singularity moving into the massive region for $a>1$.

Several open questions remain:

(i) We would like to understand the violation of the free-particle energy–momentum relation in terms of the S-matrix.

(ii) What is the meaning of the vanishing of the mass gap at the Yang–Lee branch point for large boundary factor $a>1$ in the massive phase?

(iii) We lack a derivation of the boundary exponent ρ defined in (4.2).

(iv) In the antiferromagnetic region, in a homogeneous (non-staggered) imaginary field, we find boundary condition-dependent lines where the mass gap vanishes. More work is needed to clarify the physics involved at these lines.

(v) The nature of the oscillatory phase appearing for $h>h_c$ deserves further study.

We conclude by considering the question 'can analogous square-root branch points, leading to non-unitary conformal phase transitions, appear in other quantum chain Hamiltonians too?' This will be the case if, switching on an imaginary field in the high-temperature regime, the eigenvalues of H do not become complex immediately, but stay real up to a certain finite imaginary field strength h_c. With our Hamiltonian (1.7) this happened because its characteristic polynomial had real coefficients, even with an imaginary field which rendered H non-Hermitian. Now, this feature appears also if we generalize (1.7) to a Blume–Emery–Griffiths higher-spin quantum chain with an imaginary field:

$$H=\sum_{i=1}^{N}\left(\alpha(S_i^x)^2+\beta S_i^z-S_i^xS_{i+1}^x+\mathrm{i}h_1S_i^x+\mathrm{i}h_2(S_i^x)^3+\ldots\right) \tag{6.1}$$

where S_i^x and S_i^z are spin-j matrices acting at site i.

The phase diagram of the spin-1 case of (6.1) for $h_1 = h_2 = 0$ has been given, e.g. in [43]. We have calculated the lowest-level crossings for $h_1 \neq 0$ in this model (for spin 1 the term with h_2 is not independent) in the high-temperature neighbourhood of the Ising-like critical curve. We find that the lowest-level crossing points converge to a second-order transition line on which the spectrum again suggests conformal invariance with $c = -\frac{22}{5}$. Details will be published elsewhere.

Acknowledgments

I thank Professor P K Mitter and the members of the LPTHE group for the kind hospitality at the Université Paris VI where part of this work was done Discussions with O Babelon, K Becker, M Becker, R Flume, L Kaldenbach and V Rittenberg have been very useful and stimulating. This work was supported by the PROCOPE programme of the DAAD (Deutscher Akademischer Austauschdienst).

References

[1] Yang C N and Lee T D 1952 *Phys Rev* **87** 404, 410
[2] Suzuki M 1967 *Prog Theor. Phys* **38** 1225
[3] Griffiths R B 1968 *J Math Phys* **9** 2064
[4] Asano T 1968 *Prog Theor Phys* **40** 1328. 1970 *Phys Rev Lett* **24** 1409
[5] Suzuki M and Fisher M E 1971 *J Math Phys* **12** 235
[6] Kortman P J and Griffiths R B 1971 *Phys Rev. Lett* **27** 1439
[7] Dunlop F and Newman C M 1975 *Commun Math Phys* **44** 223
[8] Bessis J D, Drouffe J M and Moussa P 1976 *J Phys A Math Gen* **9** 2105
[9] Kurtze D A and Fisher M E 1978 *J. Stat Phys* **19** 205
[10] Baker G A Jr, Fisher M E and Moussa P 1979 *Phys Rev Lett* **42** 615
[11] Moussa P 1981 *Numerical Methods in the Study of Critical Phenomena Springer Series in Synergetics* vol 9 (Berlin Springer) p 159
[12] Fisher M E 1978 *Phys Rev. Lett* **40** 1610
[13] de Alcantara Bonfin O, Kirkham J E and McKane A J 1981 *J Phys A Math Gen* **14** 2391
[14] Bander M and Itzykson C 1984 *Phys Rev* B **30** 6485
[15] Belavin A A, Polyakov A M and Zamolodchikov A B 1984 *Nucl Phys* B **241** 333
[16] Itzykson C, Saleur H and Zuber J B (ed) 1988 *Conformal Invariance and Applications to Statistical Mechanics* (Singapore World Scientific)
[17] Cardy J L 1985 *Phys Rev Lett.* **54** 1354
[18] Di Francesco P, Saleur H and Zuber J-B 1987 *Nucl. Phys* B **285** [FS19] 454, 1988 *Nucl Phys* B **300** [FS22] 393, 1987 *J Stat Phys* **49** 57
[19] Riggs H 1989 *Nucl Phys* B **326** 673
[20] Freund P G O, Klassen T R and Melzer E 1989 *Phys Lett* **229B** 243
[21] Itzykson C, Saleur H and Zuber J-B 1986 *Europhys Lett* **2** 91
[22] Zamolodchikov A B 1989 *Proc 1988 Taniguchi Symposium Kyoto, Adv Studies in Pure Math* **19** 1, 1989 *Int J Mod Phys* A **4** 4235
[23] Cardy J L 1989 *Proc. 1988 Les Houches Summer School* ed E Brezin and J Zinn-Justin (Amsterdam. North-Holland)
[24] Cardy J L and Mussardo G 1989 *Phys Lett* **B225B** 275
[25] Yurov V P and Zamolodchikov Al B 1990 *Int J Mod Phys* A **5** 3221
[26] Zamolodchikov Al B 1990 *Nucl Phys* B **342** 695
[27] Klassen T R and Melzer E 1990 *Nucl Phys* B **338** 485
[28] Klassen T R and Melzer E 1991 *Nucl Phys* B **350** 635
[29] Lassig M, Mussardo G and Cardy J L 1991 *Nucl Phys* B **348** 591
[30] Smirnov F A 1990 *Nucl Phys* B **337** 156
[31] Zamolodchikov Al B 1991 *Nucl. Phys* B **348** 619

[32] Uzelac K, Pfeuty P and Jullien R 1979 *Phys Rev Lett* **43** 805, 1979 *Phys. Rev* B **22** 436
[33] Uzelac K 1980 *Thesis* Université de Paris Sud (Orsay)
[34] Uzelac K and Jullien R 1981 *J. Phys. A Math Gen* **14** L151
[35] Jullien R, Uzelac K, Pfeuty P and Moussa P 1981 *J. Phys* **42** 1075
[36] Koberle R and Swieca J A 1979 *Phys. Lett* **86B** 209
[37] Van den Broeck J M and Schwartz L W 1979 *SIAM J. Math Anal.* **10** 639
[38] Henkel M and Schutz G 1988 *J. Phys A: Math. Gen* **21** 2617
[39] Henkel M 1990 *Finite-size Scaling and Numerical Simulation of Statistical Systems* ed V Privman (Singapore World Scientific)
[40] Affleck I 1986 *Phys Rev Lett* **56** 746
Blote H W J, Cardy J L and Nightingale M P 1986 *Phys Rev Lett* **56** 742
[41] Gehlen G V, Rittenberg V and Ruegg H 1985 *J Phys A. Math Gen.* **19** 107
[42] Henkel M and Saleur H 1989 *J Phys A Math. Gen.* **22** L513
[43] Gehlen G V 1990 *Nucl. Phys* B **330** 741
[44] Sagdeev I R and Zamolodchikov A B 1989 *Mod Phys. Lett* **3B** 1375
[45] Henkel M and Saleur H 1990 *J. Phys A. Math. Gen* **23** 791
[46] Henkel M and Ludwig A W W 1990 *Phys. Lett.* **249B** 463
[47] Alcaraz F 1990 *J. Phys A Math Gen* **23** L1105
[48] Henkel M 1991 *J Phys A. Math Gen* **24** L133
[49] Lauwers P and Rittenberg V 1989 *Phys Lett.* **233B** 197
[50] Lauwers P and Schutz G 1991 *Phys. Lett* **256B** 491
[51] Lieb E, Schultz T and Mattis D 1961 *Ann Phys* **16** 407
[52] Hamer C J and Barber M N 1981 *J Phys. A. Math Gen* **14** 241
[53] Burkhardt T W and Guim I 1986 *J Phys. A: Math Gen* **18** L33
[54] Henkel M 1987 *J Phys A: Math. Gen* **20** 995
[55] Cardy J L 1988 *Phys Rev Lett* **60** 2709
[56] Lüscher M 1989 *Proc 1988 Les Houches Summer School* ed E Brezin and J Zinn-Justin (Amsterdam North-Holland)
[57] Luscher M and Wolff U 1990 *Nucl Phys* B **339** 222
[58] McCoy B, Tracy C A and Wu T T 1977 *Phys Rev Lett* **38** 793
[59] Sato M, Miwa T and Jimbo M 1977 *Proc. Japan Acad* **53A** 219
[60] Schroer B and Truong T T 1978 *Nucl Phys* B **144** 80
[61] Lassig M and Martins M J 1991 *Nucl Phys* B **354** 666
[62] Klassen T R and Melzer E 1991 *Nucl Phys.* B **362** 329
[63] Henkel M, Patkos A and Schlottmann M 1989 *Nucl Phys.* B **314** 609
[64] Baake M, Chaselon P and Schlottmann M 1989 *Nucl Phys.* B **314** 625
[65] Grimm U 1990 *Nucl Phys* B **340** 633
[66] Grimm U and Rittenberg V 1991 *Nucl Phys.* B **354** 418
[67] Baranowski D and Rittenberg V 1990 *J Phys A Math Gen* **23** 1029